Research Article

Michaelis-Menten-Type Prey Harvesting in Discrete Modified Leslie-Gower Predator-Prey Model

M. Saqib Khan,[1,2] **Mujahid Abbas,**[1,3] **Ebenezer Bonyah** [ID],[4] **and Hengxiao Qi**[5,6]

[1]*Department of Mathematics, Government College University, Lahore 54000, Pakistan*
[2]*Department of Mathematics, Riphah International University - Lahore Campus, Islamabad, Pakistan*
[3]*Department of Medical Research, China Medical University, Taichung 40402, Taiwan*
[4]*Department of Mathematics Education, Akenten Appiah Menka University of Skills Training and Entrepreneurial Development, Kumasi, Ghana*
[5]*Party School of Shandong Provincial Committee of the Communist Party of China (Shandong Administration College), Jinan 250014, China*
[6]*The Research Center of Theoretical System of Socialism with Chinese Characteristics in Shandong Province, Jinan 250014, China*

Correspondence should be addressed to Ebenezer Bonyah; ebbonya@gmail.com

A discrete-time Michaelis-Menten-type prey harvesting is discussed in this paper, in the modified Leslie-Gower predator-prey model. Detailed analysis of the topology of nonnegative interior fixed points is given, including their existence and stability dynamics. Also, the conditions for the existence of flip and Neimark-Sacker bifurcations are derived by using the center manifold theorem and bifurcation theory. The numerical simulations are provided, using a computer package, to illustrate the consistency of theoretical results.

1. Introduction

The basic interaction between various species on this planet is predation and is widely present in nature. The existence of most species in our ecosystem is based on predator-prey relationships, which makes the rich biodiversity of complex ecosystems possible [1]. These complexities can aptly be explained using mathematical models and the related dynamics. As Clark has observed in [2], the dynamics of the predator-prey models also provide methods to optimally manage renewable resources, apart from coexistence conditions of predators and preys. For this ecosystem, the most basic model was proposed by Lotka [3] and Volterra [4], in early 20th century. This model captured the oscillating behavior in populations of a predator and its prey. The simplicity of this model, however, is unable to address most real-world scenarios. To rectify this, many modifications of Lotka-Volterra type model have been proposed by researchers. In [5], Holling proposed various types of functional responses to better understand the components of predator-prey interactions.

An alternative was proposed by Leslie, in [6], in which the number of prey and the carrying capacity of the predator's environment was proportional. Leslie focused on the fact that the increasing capacity of both predator and prey cannot be unbounded. This fact was not incorporated in the Lotka-Volterra model. This model was shown, in [7], to possess globally asymptotically stable and unique positive equilibrium, for any permissible parameters. Then, May in [8] showed its stability with Holling functional responses. L. Chen and F. Chen proved the global stability of the unique interior equilibrium for a Leslie-Gower predator-prey model with feedback controls [9]. Uniqueness of limit cycles and the Hopf bifurcation for this model was discussed in [10, 11].

The primary drawback of this model is that if the prey population is at low densities, it is not possible for the predator to switch to alternative food source [12]. Aziz-Alaoui and Daher [13] rectified this scenario by adding a

provisional alternative food source parameter. This model is generally called the modified Leslie-Gower predator-prey model. Caughley [14] modelled the biological control of the prickly-pear cactus by the moth Cactoblastis cactorum, using this system. In [15, 16], the authors used this system to model the predator-prey mite outbreak interactions on fruit trees. Much work has been done on this model. For further details, look at [17–23] and the references therein. In [24], W. C. Allee introduced what was altered termed as the Allee effects, to the Leslie-Gower type models. The stability dynamics and bifurcation analysis of the predator-prey systems subject to Allee effect is discussed in [25–28].

Harvesting of different biological species is necessary for a variety of reasons. The ever-increasing use of natural resources, either due to the increase in human population or in the name of economic progress, has caused the ecological system of this planet to trip from the equilibrium it was in, for thousands of years. A common outcome of these practices is the extinction of species from the face of this planet. Harvesting of such species is one way to minimize the damage. Harvesting for species is also practices for purely business reasons. But there is a silver lining in this strategy. The more harvesting is done, the more predator species are likely to become extinct [29]. Thus, the need to reinforce scientific management of harvesting is much needed. Clark [2] discussed the problem of combined or nonselective harvesting of two ecologically independent populations obeying the logistic law of growth. Multispecies harvesting models are studied in detail by Chaudhuri [30, 31], Mesterton-Gibbons [32], Kar and Chaudhuri [33, 34], etc. Nonselective harvesting model of a prey-predator fishery is studied in detail by Chaudhuri and Ray [35], Kar et al. [36], etc.

Michaelis-Menten-type predator-prey model, alternatively known as the ratio-dependent predator-prey model, uses the idea that the ratio of prey to predator abundance directly affects the per capita predator growth rate. The effectiveness of this model is backed by a plethora of experimental and observational data, for the predator which must compete for prey. For more details, see ([37–43]). Michaelis-Menten-type predator-prey model has been rigorously studied in ([44–49]) and references therein. This investigation discovered existence of rich dynamics, like stable limit cycle, multiple attractors, and deterministic extinction, to name a few. Existence of hyperbolic, parabolic, and elliptic orbits was revealed near the origin, as well as combinations of such orbits, for various parametric values.

The continuous predator-prey models have been successfully used to obtain desired results, and the disadvantages of using continuous systems are also quite apparent. By definition, the continuous systems require the subject species have continuous and overlapping generations. This is not generally true, for example, salmon, which have an annual spawning season and are born at the same time each year. For these types of populations which have nonoverlapping generation characteristics, the discrete time models are more descriptive and suitable than the continuous models [50]. Also, the discrete models should generate richer and reality-based dynamics compared to the continuous time models [51]. In addition, since many continuous models cannot be solved analytically, using difference equations for approximation and finding solution is much practical way to approach the problem. In population biology and complex ecosystems, discrete-time models are used to examine the taxonomic group of organisms and species with the passage of time. These models are best to describe the chaotic behavior of nonlinear dynamics [52, 53].

Gupta and Chandra, in [54], proposed and studied modified Leslie-Gower predator-prey model with Michaelis-Menten-type prey harvesting in prey. They proved the permanence and stability and discuss different bifurcations of this model. Their model guaranteed a feasible upper bound of the rate of harvesting for the coexistence of the species. Their model is given in [54] as

$$\frac{dx}{dt} = x\left(1 - x - \frac{\alpha y}{m + x} - \frac{h}{c + x}\right), \tag{1}$$

$$\frac{dy}{dt} = \rho y\left(1 - \frac{\beta y}{m + x}\right), \tag{2}$$

with the initial conditions $x(0) > 0$, $y(0) > 0$. Here, $x(t)$ and $y(t)$ represent prey and predator densities, respectively, at time t. The details of the parameters are given in their paper. For our purposes, all parameters are positive.

Another possible way to understand the complex problem of interaction between prey and predator is by using discrete models. We use the forward Euler method to discretize the above system. The discrete counterpart of (1) can be given as

$$x_{n+1} = x_n + kx_n\left(1 - x_n - \frac{\alpha y_n}{m + x_n} - \frac{h}{c + x_n}\right), \tag{3}$$

$$y_{n+1} = y_n + k\rho y_n\left(1 - \frac{\beta y_n}{m + x_n}\right). \tag{4}$$

In the remainder of this paper, we present the discrete counterpart of the Michaelis-Menten-type prey harvesting in modified Leslie-Gower predator-prey model, ((4)). Our aim is to illustrate the detailed mathematical analysis of the topology of nonnegative interior fixed points, including their existence in Section 2 and stability dynamics in Section 3. The conditions for the existence of flip and Neimark-Sacker bifurcations will be derived in Section 4, using the center manifold theorem and bifurcation theory. The theory will be verified through numerical examples in Section 5. Finally, we will conclude in Section 6.

2. The Fixed Points

In order to find the fixed points, we need to solve the following system.

$$x\left(1 - x - \frac{\alpha y}{m + x} - \frac{h}{c + x}\right) = 0, \tag{5}$$

$$y\left(1 - \frac{\beta y}{m + x}\right) = 0. \tag{6}$$

The system has four fixed points on the boundary, namely,

$$\{E_1, E_2, E_{3,4}\} = \left\{(0,0), \left(0, \frac{m}{\beta}\right), \left(\frac{1 - c \pm \sqrt{(c+1)^2 - 4h}}{2}, 0\right)\right\}. \tag{7}$$

For positive equilibrium points, we have the following cases.

(i) The system has no positive stationary point, if

$$(\alpha - \beta(c+1))^2 < 4\beta^2 h \tag{8}$$

(ii) If $(\alpha - \beta(c+1))^2 = 4\beta^2 h$, then the system has a unique positive stationary point, $E_* = (x^*, m + x^*/\beta)$, where

$$x^* = \frac{1}{2}\left(1 - c - \frac{\alpha}{\beta}\right) \tag{9}$$

(iii) If $(\alpha - \beta(c+1))^2 > 4\beta^2 h$, the system will have two positive stationary points $E_5 = (x_m, m + x_m/\beta)$ and $E_6 = (x_p, m + x_p/\beta)$, where

$$x_m = \frac{-\alpha + \beta(1-c) - \sqrt{(\alpha - \beta(c+1))^2 - 4\beta^2 h}}{2\beta}$$

$$x_p = \frac{-\alpha + \beta(1-c) + \sqrt{(\alpha - \beta(c+1))^2 - 4\beta^2 h}}{2\beta}$$

$$\tag{10}$$

As can be seen in Figure 1, the positive interior points may vanish or merge into one another, depending on the values of parameters.

3. The Topological Dynamics of the Fixed Points

The respective Jacobian matrices, evaluated at each fixed point, are

$$J_1 = \begin{bmatrix} 1 + k\left(1 - \frac{h}{c}\right) & 0 \\ 0 & 1 + k\rho \end{bmatrix}$$

$$J_2 = \begin{bmatrix} 1 + k\left(1 - \frac{h}{c} - \frac{\alpha}{\beta}\right) & 0 \\ k\frac{\rho}{\beta} & 1 - k\rho \end{bmatrix}$$

$$J_{3,4} = \begin{bmatrix} 1 + kx\left(-1 + \frac{1-x}{c+x} - \frac{\alpha}{\beta}\right) & -k\frac{x\alpha}{m+x} \\ 0 & 1 + k\rho \end{bmatrix}$$

$$J_{*,5,6} = \begin{bmatrix} 1 + kA_1 & -kA_2 \\ kA_3 & 1 - kA_4 \end{bmatrix}, \tag{11}$$

where

$$A_1 = x\left(\frac{h}{(c+x)^2} + \frac{\alpha y}{(m+x)^2} - 1\right),$$

$$A_2 = \frac{\alpha x}{m+x}, \tag{12}$$

$$A_3 = \frac{\rho y}{m+x},$$

$$A_4 = \rho.$$

In order to find the topology and properties of the aforementioned fixed points, the following lemma will be used, which is omnipresent in the text books related to discrete dynamical systems.

Lemma 1. *Let $t_i = Tr(J_i)$, $det_i = |J_i|$, and $p_i(z) = z^2 - t_i z + det_i$, $i \in \{1, 2, 3, 4, *, 5, 6\}$. Suppose z_1 and z_2 are the roots of $p(z)$. Then,*

(i) $|z_{1,2}| < 1$ *if and only if $p(-1) > 0$ and $\det < 1$*

(ii) $|z_{1,2}| > 1$ *if and only if $p(-1) > 0$ and $\det > 1$*

(iii) $|z_1| < 1$ *and $|z_2| > 1$ (or vice versa) if and only if $p(-1) < 0$*

(iv) $z_1 = -1$ *and $|z_2| \neq 1$ if and only if $p(-1) = 0$ and $t \neq -2, 0$*

(v) $z_{1,2}$ *are complex, and $|z_{1,2}| = 1$ if and only if $4 \det - t^2 > 0$ and $\det = 1$*

If z_1 and z_2 are the eigenvalues of 2×2 Jacobian matrix, then,

Lemma 2. *A fixed point E_i, $i \in \{1, 2, 3, 4, *, 5, 6\}$ is called*

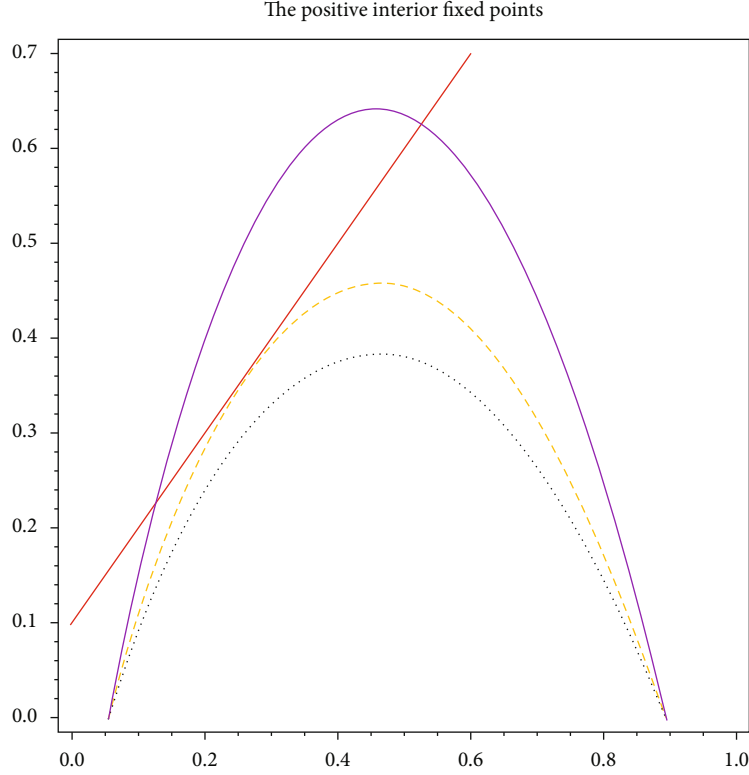(i) *Sink if $|z_1| < 1$ and $|z_2| < 1$, so sink is locally asymptotically stable*

FIGURE 1: The purple graph is for $\alpha = 0.3, h = 0.1, m = 0.1, c = 0.05, \beta = 1, \rho = 2.6$, which is showing two positive fixed points. The brown dashed graph is for $\alpha = 0.42, h = 0.1, m = 0.1, c = 0.05, \beta = 1, \rho = 2.6$, which is showing unique positive fixed point. The black dotted graph is for $\alpha = 0.5, h = 0.1, m = 0.1, c = 0.05, \beta = 1, \rho = 2.6$, which is showing no positive fixed point.

(ii) *Source if $|z_1| > 1$ and $|z_2| > 1$, so source is locally unstable*

(iii) *Saddle if $|z_1| < 1$ and $|z_2| > 1$ (or $|z_1| > 1$ and $|z_2| < 1$)*

(iv) *Nonhyperbolic if either $|z_1| = 1$ or $|z_2| = 1$*

Using the above lemma, we can easily see that E_1 is saddle if $c < h$ and unstable if $c > h$. If $h = c$, then it may undergo transcritical or fold bifurcation, and if $h = c(1 + 2/k)$, it undergoes period-doubling bifurcation. Similarly, the fixed representing the prey free scenario, E_2, is saddle if $h < c(1 - \alpha/\beta)$ and stable if $h > c(1 - \alpha/\beta)$. If $h = c(1 - \alpha/\beta)$, then it may undergo transcritical or fold bifurcation, and if $h = c(1 - \alpha/\beta + 2/k)$, it undergoes period-doubling bifurcation. The fixed points, representing the extinction of predator, $E_{3,4}$, are saddle if $h < (c + \bar{x})^2$ and unstable if $h > (c + \bar{x})^2$. If $h = (c + \bar{x})^2$, then these fixed points may undergo transcritical or fold bifurcation, and if $h = (1 - 2/k\bar{x})(c + \bar{x})^2$, the fixed points undergo period-doubling bifurcation. For all these boundary fixed points, Neimark-Sacker bifurcation is not possible.

We are much more interested in the behavior of interior fixed points, which are much more richer in comparison and for practical purposes, usable.

Theorem 3. *For the fixed points E_*, E_5, and E_6, if $\beta \geq A_2/A_1$ then let $\rho > 0$, and if $\beta < A_2/A_1$, then let $\rho \notin (\rho_1, \rho_2)$, where*

$$\rho_1 = \frac{-(\beta A_1 - 2A_2) - 2\sqrt{A_2(A_2 - A_1\beta)}}{\beta},$$

$$\rho_2 = \frac{-(\beta A_1 - 2A_2) + 2\sqrt{A_2(A_2 - A_1\beta)}}{\beta}. \tag{13}$$

If

$$k_1 = \frac{A_1 - A_4 - \sqrt{(A_1 + A_4)^2 - 4A_2A_3}}{A_1A_4 - A_2A_3},$$

$$k_2 = \frac{A_1 - A_4 + \sqrt{(A_1 + A_4)^2 - 4A_2A_3}}{A_1A_4 - A_2A_3}. \tag{14}$$

Then,

(1) *The fixed points are locally asymptotically stable if $k \in (0, k_1)$*

(2) *The fixed points are locally unstable if $k \in (k_2, \infty)$*

(3) *The fixed points are saddle if $k \in (k_1, k_2)$*

(4) *The fixed points are nonhyperbolic with eigenvalues $z_1 = 1$ and $|z_2| \neq 1$, if and only if $h = (c + \bar{x})^2$*

(5) *The fixed points are nonhyperbolic with eigenvalues $z_1 = -1$ and $|z_2| \neq 1$, if $k \in \{k_1, k_2\}$ and $k \notin \{2/A_4 - A_1, 4/A_4 - A_1\}$*

(6) *The fixed points are nonhyperbolic, having complex conjugate eigenvalues, with $|z_1| = 1 = |z_2|$ if and only if $k = A_1 - A_4/A_1A_4 - A_2A_3$ and $k \in (0, 4/A_4 - A_1)$*

Proof. For any positive interior fixed point, E_*, E_5, or E_6, the characteristic polynomial of the Jacobian matrix at the given fixed point is

$$p(z) = z^2 - tz + \det, \tag{15}$$

where $t = 2 + (A_1 - A_4)k$ and $\det = (A_2A_3 - A_1A_4)k^2 + (A_1 - A_4)k + 1$. Then, we can use Lemma 1, since for any $k > 0$,

$$p(1) = 1 - t + \det = (A_2A_3 - A_1A_4)k^2. \tag{16}$$

Thus, $p(1) = 0$ if $h/(c + x)^2 - 1 = 0$, or

$$h = (c + x)^2. \tag{17}$$

Also,

$$p(-1) = (A_2A_3 - A_1A_4)k^2 + 2(A_1 - A_4)k + 4, \tag{18}$$

which shows that

$$\begin{cases} p(-1) > 0 & k \in (0, k_1) \cup (k_2, \infty), \\ p(-1) < 0 & k \in (k_1, k_2), \\ p(-1) = 0 & k \in \{k_1, k_2\}. \end{cases} \tag{19}$$

Also,

$$\begin{cases} \det > 1 & k \in \left(\dfrac{A_1 - A_4}{A_1A_4 - A_2A_3}, \infty \right), \\ \det < 1 & k \in \left(0, \dfrac{A_1 - A_4}{A_1A_4 - A_2A_3} \right), \\ \det = 1 & k = \dfrac{A_1 - A_4}{A_1A_4 - A_2A_3}. \end{cases} \tag{20}$$

Then, using Lemmas 1 and 2, we have the following results.

(1) Each fixed point is a sink if and only if

$$k \in \{(0, k_1) \cup (k_2, \infty)\} \cap \left(0, \frac{A_1 - A_4}{A_1A_4 - A_2A_3} \right) = (0, k_1) \tag{21}$$

(2) Each fixed point is a source if and only if

$$k \in \{(0, k_1) \cup (k_2, \infty)\} \cap \left(\frac{A_1 - A_4}{A_1A_4 - A_2A_3}, \infty \right) = (k_2, \infty) \tag{22}$$

(3) Each fixed point is saddle if and only if $k \in (k_1, k_2)$

(4) The Jacobian matrix at the given fixed points has eigenvalues $z_1 = 1$ and $|z_2| \neq 1$ if and only if $h = (c + \bar{x})^2$

(5) The Jacobian matrix at the given fixed points has eigenvalues $z_1 = -1$ and $|z_2| \neq 1$, if and only if $k = k_1$ or $k = k_2$ and $h \neq 2/A_4 - A_1$ and $h \neq 4/A_4 - A_1$

(6) The eigenvalues are complex conjugates with $|z_1| = 1 = |z_2|$ if and only if $k = A_1 - A_4/A_1A_4 - A_2A_3$ and $k \in (0, 4/A_4 - A_1)$

□

Remark 4. As used in [55, 56], we know that due to the jury condition, a transcritical or fold bifurcation is obtained when $p_j(1) = 0$, $j \in \{*, 5, 6\}$. As shown above, this is only true if $h = (c + \bar{x})^2$. For the fixed point E^*, this condition is equivalent to $h = 1/4(\alpha/\beta - c - 1)^2$, which we gets automatically, since in this scenario, $(\alpha/\beta - c - 1)^2 - 4h = 0$. Thus, we always have $p_*(1) = 0$ for the fixed point E^*, i.e., a transcritical or fold bifurcation is always obtained for any parametric values, at the fixed point E^*.

4. Bifurcations

For positive fixed points, E_5 and E_6, define

$$\Omega_{PD} = \left\{ (\alpha, \beta, h, m, c, \rho, k_0) \in \mathbb{R}_+^7 : k_0 = k_1 \text{or} k_2, k_0 \right.$$
$$\left. \neq \frac{2}{A_4 - A_1}, k_0 \neq \frac{4}{A_4 - A_1}, \rho \notin (\rho_1, \rho_2) \right\},$$

$$\Omega_{NS} = \left\{ (\alpha, \beta, h, m, c, \rho, k_0) \in \mathbb{R}_+^7 : k_0 \right.$$
$$\left. = \frac{A_1 - A_4}{A_1A_4 - A_2A_3}, k \in \left(0, \frac{4}{A_4 - A_1} \right) \right\}. \tag{23}$$

The procedure is identical for finding the normal form of the bifurcations for E_5 and E_6, as illustrated below.

4.1. Period-Doubling Bifurcation. Let $(\alpha, \beta, h, m, c, \rho, k_0) \in \Omega_{PD}$ and let K denote the perturbation parameter for the mapping (3), i.e., $|K| \ll 1$. Then, variation of parameters in small neighborhood of Ω_{PD} gives emergence of period

doubling bifurcation. Let k_0 be the bifurcation parameter. The perturbed mapping is

$$\begin{pmatrix} x \\ y \end{pmatrix} \longrightarrow \begin{pmatrix} x + (k+K)x\left(1 - x - \dfrac{\alpha y}{m+x} - \dfrac{h}{c+x}\right) \\ y + (k+K)\rho y\left(1 - \dfrac{\beta y}{m+x}\right) \end{pmatrix}. \tag{24}$$

Define $X = x - \bar{x}$ and $Y = y - \bar{y}$, to translate the fixed point to $(0, 0)$. Here, $(\bar{x}, \bar{y})$ is the positive interior fixed point. Then, the above mapping is converted to

$$\begin{pmatrix} X \\ Y \end{pmatrix} \longrightarrow \begin{pmatrix} X + (k+K)(X+\bar{x})\left(1 - (X+\bar{x}) - \dfrac{\alpha(Y+\bar{y})}{m+(X+\bar{x})} - \dfrac{h}{c+(X+\bar{x})}\right) \\ Y + (k+K)\rho(Y+\bar{y})\left(1 - \dfrac{\beta(Y+\bar{y})}{m+(X+\bar{x})}\right) \end{pmatrix}. \tag{25}$$

After Taylor series expansion, the above mapping can be written as

$$\begin{pmatrix} X \\ Y \end{pmatrix} \longrightarrow \begin{pmatrix} a_{11} & a_{12} \\ a_{21} & a_{22} \end{pmatrix} \begin{pmatrix} X \\ Y \end{pmatrix} + \begin{pmatrix} f_{PD}(X, Y, K) \\ g_{PD}(X, Y, K) \end{pmatrix}, \tag{26}$$

where $a_{11} = 1 + kA_1$, $a_{12} = -kA_2$, $a_{21} = kA_3$, and $a_{22} = 1 - kA_4$, and

$$\begin{aligned} f_{PD}(X, Y, K) = {} & kb_1X^2 + kb_2XY + A_1KX - A_2KY + kb_3Y^2 \\ & + kb_4X^3 + kb_5X^2Y + b_1KX^2 + b_2KXY \\ & + b_3KY^2 + kb_6XY^2 + kb_7Y^3 \\ & + O\left(|X + Y + K|^4\right), \end{aligned}$$

$$\begin{aligned} g_{PD}(X, Y, K) = {} & kb_8X^2 + kb_9XY + A_3KX - A_4KY + kb_{10}Y^2 \\ & + kb_{11}X^3 + kb_{12}X^2Y + b_8KX^2 + b_9KXY \\ & + b_{10}KY^2 + kb_{13}XY^2 + kb_{14}Y^3 \\ & + O\left(|X + Y + K|^4\right), \end{aligned} \tag{27}$$

and

$$b_1 = \frac{ch}{(c+\bar{x})^3} + \frac{\alpha m\bar{y}}{(m+\bar{x})^3} - 1,$$

$$b_2 = -\frac{\alpha m}{(m+\bar{x})^2},$$

$$b_3 = 0$$

$$b_4 = -\frac{ch}{(c+\bar{x})^4} - \frac{\alpha m\bar{y}}{(m+\bar{x})^4},$$

$$b_5 = \frac{\alpha m}{(m+\bar{x})^3},$$

$$b_6 = 0,$$

$$b_7 = 0,$$

$$b_8 = -\frac{\rho\bar{y}}{(m+\bar{x})^2},$$

$$b_9 = \frac{2\rho}{m+\bar{x}},$$

$$b_{10} = -\frac{\beta\rho}{m+\bar{x}},$$

$$b_{11} = \frac{\rho\bar{y}}{(m+\bar{x})^3},$$

$$b_{12} = -\frac{2\rho}{(m+\bar{x})^2},$$

$$b_{14} = 0 \qquad b_{13} = \frac{\beta\rho}{(m+\bar{x})^2}, \tag{28}$$

To convert the system (43) in the normal form, let

$$\begin{aligned} \begin{pmatrix} X \\ Y \end{pmatrix} = T_{PD} \begin{pmatrix} u \\ v \end{pmatrix} & = \begin{pmatrix} a_{12} & a_{12} \\ z_1 - a_{11} & z_2 - a_{22} \end{pmatrix} \begin{pmatrix} u \\ v \end{pmatrix} \\ & = \begin{pmatrix} a_{12} & a_{12} \\ -1 - a_{11} & z_2 - a_{22} \end{pmatrix} \begin{pmatrix} u \\ v \end{pmatrix}, \end{aligned} \tag{29}$$

where T_{PD} is an invertible matrix. Thus, we can convert the above system, such that we have $(0, 0)$ as fixed points, as shown below.

$$\begin{aligned} \begin{pmatrix} u \\ v \end{pmatrix} \longrightarrow {} & \begin{pmatrix} -1 & 0 \\ 0 & z_2 \end{pmatrix} \begin{pmatrix} u \\ v \end{pmatrix} + T_{PD}^{-1} \begin{pmatrix} f_{PD}(u, v, K) \\ g_{PD}(u, v, K) \end{pmatrix} \\ \longrightarrow {} & \begin{pmatrix} -1 & 0 \\ 0 & z_2 \end{pmatrix} \begin{pmatrix} u \\ v \end{pmatrix} + \begin{pmatrix} \tilde{f}_{PD}(u, v, K) \\ \tilde{g}_{PD}(u, v, K) \end{pmatrix}, \end{aligned} \tag{30}$$

where

$$\tilde{f}_{PD}(u, v, K) = d_1 u^2 + d_2 uv + d_3 Ku + d_4 Kv + d_5 v^2 + d_6 u^3$$
$$+ d_7 u^2 v + d_8 Ku^2 + d_9 Kuv + d_{10} Kv^2 + d_{11} uv^2$$
$$+ d_{12} v^3 + O\left(|u + v + K|^4\right),$$

$$\tilde{g}_{PD}(u, v, K) = d_{13} u^2 + d_{14} uv + d_{15} Ku + d_{16} Kv + d_{17} v^2$$
$$+ d_{18} u^3 + d_{19} u^2 v + d_{20} Ku^2 + d_{21} Kuv$$
$$+ d_{22} Kv^2 + d_{23} uv^2 + d_{24} v^3 + O\left(|u + v + K|^4\right),$$
(31)

and

$$d_1 = c_1 k\left(a_{12}(a_{11} + 1)(b_9 - b_2 c_2) + a_{12}^2(b_1 c_2 - b_8) + (a_{11} + 1)^2(-b_{10})\right),$$

$$d_2 = c_1(-k)\left(-a_{12}(a_{11} + a_{22} - z_2 + 1)(b_9 - b_2 c_2) + 2a_{12}^2(b_8 - b_1 c_2) + 2(a_{11} + 1)b_{10}(a_{22} - z_2)\right),$$

$$d_3 = c_1(a_{12}(A_1 c_2 + A_3) + (a_{11} + 1)(A_2 c_2 - A_4)),$$

$$d_4 = c_1((a_{22} - z_2)(A_2 c_2 - A_4) + a_{12}(A_1 c_2 + A_3)),$$

$$d_5 = c_1 k\left(a_{12}(a_{22} - z_2)(b_9 - b_2 c_2) + a_{12}^2(b_1 c_2 - b_8) - b_{10}(a_{22} - z_2)^2\right),$$

$$d_6 = c_1 k\left(a_{12}^3(b_4 c_2 - b_{11}) + (a_{11} + 1)a_{12}^2(b_{12} - b_5 c_2) - (a_{11} + 1)^2 a_{12} b_{13}\right),$$

$$d_7 = c_1 k\left(a_{12}^2(2a_{11} + a_{22} - z_2 + 2)(b_{12} - b_5 c_2) - 3a_{12}^3(b_{11} - b_4 c_2) - (a_{11} + 1)a_{12} b_{13} \cdot (a_{11} + 2a_{22} - 2z_2 + 1)\right),$$

$$d_8 = c_1\left(a_{12}(a_{11} + 1)(b_9 - b_2 c_2) + a_{12}^2(b_1 c_2 - b_8) + (a_{11} + 1)^2(-b_{10})\right),$$

$$d_9 = -c_1\left(-a_{12}(a_{11} + a_{22} - z_2 + 1)(b_9 - b_2 c_2) + 2a_{12}^2(b_8 - b_1 c_2) + 2(a_{11} + 1)b_{10}(a_{22} - z_2)\right),$$

$$d_{10} = c_1\left(a_{12}(a_{22} - z_2)(b_9 - b_2 c_2) + a_{12}^2(b_1 c_2 - b_8) - b_{10}(a_{22} - z_2)^2\right),$$

$$d_{11} = c_1 k\left(a_{12}^2(a_{11} + 2a_{22} - 2z_2 + 1)(b_{12} - b_5 c_2) - 3a_{12}^3(b_{11} - b_4 c_2) - a_{12} b_{13}(a_{22} - z_2) \cdot (2a_{11} + a_{22} - z_2 + 2)\right),$$

$$d_{12} = c_1 k\left(a_{12}^2(a_{22} - z_2)(b_{12} - b_5 c_2) + a_{12}^3(b_4 c_2 - b_{11}) - a_{12} b_{13}(a_{22} - z_2)^2\right),$$

$$d_{13} = c_1 k\left(a_{12}(a_{11} + 1)(-b_2 c_3 - b_9) + a_{12}^2(b_1 c_3 + b_8) + (a_{11} + 1)^2 b_{10}\right),$$

$$d_{14} = c_1(-k)\left(a_{12}(a_{11} + a_{22} - z_2 + 1)(b_2 c_3 + b_9) - 2a_{12}^2(b_1 c_3 + b_8) - 2(a_{11} + 1)b_{10}(a_{22} - z_2)\right),$$

$$d_{15} = c_1(a_{12}(A_1 c_3 + A_3) + (a_{11} + 1)(A_2 c_3 - A_4)),$$

$$d_{16} = c_1((a_{22} - z_2)(A_2 c_3 - A_4) + a_{12}(A_1 c_3 + A_3)),$$

$$d_{17} = c_1 k\left(-a_{12}(a_{22} - z_2)(b_2 c_3 + b_9) + a_{12}^2(b_1 c_3 + b_8) + b_{10}(a_{22} - z_2)^2\right),$$

$$d_{18} = c_1 k\left(a_{12}^3(b_4 c_3 + b_{11}) - (a_{11} + 1)a_{12}^2(b_5 c_3 + b_{12}) + (a_{11} + 1)^2 a_{12} b_{13}\right),$$

$$d_{19} = c_1 k\left(-a_{12}^2(2a_{11} + a_{22} - z_2 + 2)(b_5 c_3 + b_{12}) + 3a_{12}^3(b_4 c_3 + b_{11}) + (a_{11} + 1)a_{12} b_{13} \cdot (a_{11} + 2a_{22} - 2z_2 + 1)\right),$$

$$d_{20} = c_1\left(-a_{12}(a_{11} + 1)(b_2 c_3 + b_9) + a_{12}^2(b_1 c_3 + b_8) + (a_{11} + 1)^2 b_{10}\right),$$

$$d_{21} = -c_1\left(a_{12}(a_{11} + a_{22} - z_2 + 1)(b_2 c_3 + b_9) - 2a_{12}^2(b_1 c_3 + b_8) - 2(a_{11} + 1)b_{10}(a_{22} - z_2)\right),$$

$$d_{22} = c_1\left(-a_{12}(a_{22} - z_2)(b_2 c_3 + b_9) + a_{12}^2(b_1 c_3 + b_8) + b_{10}(a_{22} - z_2)^2\right),$$

$$d_{23} = c_1 k\left(-a_{12}^2(a_{11} + 2a_{22} - 2z_2 + 1)(b_5 c_3 + b_{12}) + 3a_{12}^3(b_4 c_3 + b_{11}) + a_{12} b_{13}(a_{22} - z_2) \cdot (2a_{11} + a_{22} - z_2 + 2)\right),$$

$$d_{24} = c_1 k\left(-a_{12}^2(a_{22} - z_2)(b_5 c_3 + b_{12}) + a_{12}^3(b_4 c_3 + b_{11}) + a_{12} b_{13}(a_{22} - z_2)^2\right) \text{ and } X = a_{12}(u + v), Y$$
$$= -(1 + a_{11})u + (z_2 - a_{22})v.$$
(32)

In order to implement the center manifold theorem, we assume that M_C be the center manifold of (30), evaluated at $(0, 0)$ in a small neighborhood of $K = 0$. It can be approximated as follows.

$$M_C = \{(K, u, v): v = G_{PD}(K, u), |u| < \delta_1, |K| < \delta_2, G_{PD}(0, 0) = 0, DG_{PD}(0, 0) = 0\},$$
(33)

where

$$F_{PD}(K, G_{PD}(K, u)) = G_{PD}\left(K, z_1 u + \tilde{f}_{PD}(K, u, G_{PD}(K, u))\right)$$
$$- z_2 G_{PD}(K, u) - \tilde{g}_{PD}(K, u, G_{PD}(K, u))$$
$$= G_{PD}\left(K, -u + \tilde{f}_{PD}(K, u, G_{PD}(K, u))\right)$$
$$- z_2 G_{PD}(K, u) - \tilde{g}_{PD}(K, u, G_{PD}(K, u)).$$
(34)

We need to find $G_{PD}(K, u)$ such that $F_{PD}(K, G_{PD}(K, u)) = 0$. Since we need the conditions in M_C to be satisfied, we may assume

$$G_{PD}(K, u) = m_1 u^2 + m_2 K u + m_3 K^2 + O(|K + u|^3). \quad (35)$$

Thus, we can write

$$F_{PD}(K, G_{PD}(K, u)) = (m_1(1 - z_2) - d_{13})u^2$$
$$- (d_{15} + m_2(z_2 + 1))Ku \quad (36)$$
$$+ m_3(1 - z_2)K^2 + O(|K + u|^3).$$

By comparing coefficients in the equation $F_{PD}(K, G_{PD}(K, u)) = 0$, we get

$$m_1 = \frac{d_{13}}{1 - z_2},$$
$$m_2 = -\frac{d_{15}}{1 + z_2}, \quad (37)$$
$$m_3 = 0,$$

and

$$G_{PD}(K, u) = \frac{d_{13}}{1 - z_2} u^2 - \frac{d_{15}}{1 + z_2} Ku + O(|K + u|^3). \quad (38)$$

The dynamics restricted to M_C are given locally by the map

$$F_C : u \mapsto z_1 u + \tilde{f}_{PD}(K, u, G_{PD}(K, u))$$
$$= -u + d_1 u^2 + d_3 Ku - \frac{d_4 d_{15}}{1 + z_2} K^2 u$$
$$+ \left(d_8 - \frac{d_4 d_{13}}{1 - z_2} - \frac{d_2 d_{15}}{1 + z_2}\right) Ku^2 \quad (39)$$
$$+ \left(d_6 + \frac{d_2 d_{13}}{1 - z_2}\right) u^3 + O(|K + u|^4).$$

Furthermore, define

$$Y_1 = \left(\frac{\partial^2 F_C}{\partial K \partial u} + \frac{1}{2} \frac{\partial F_C}{\partial K} \frac{\partial^2 F_C}{\partial u^2}\right)_{(0,0)} = d_3 \neq 0,$$

$$Y_2 = \left(\frac{1}{6} \frac{\partial^3 F_C}{\partial u^3} + \left(\frac{1}{2} \frac{\partial^2 F_C}{\partial u^2}\right)^2\right)_{(0,0)} = d_1^2 + d_6 + \frac{d_2 d_{13}}{1 - z_2} \neq 0.$$
(40)

Theorem 5. *If $Y_1 \neq 0$ and $Y_2 \neq 0$, then system undergoes period-doubling bifurcation at the unique positive equilibrium point when parameter k varies in small neighborhood of k_1 or k_2. Moreover, the period-two orbits that bifurcate from positive equilibrium are stable if $Y_2 > 0$ and unstable if $Y_2 < 0$.*

Remark 6. Since we have already found the center manifold for our system in (39), we can easily show the existence of transcritical or fold bifurcation, when one of the eigenvalue equals 1 and the other not on the unit circle.

4.2. Neimark-Sacker Bifurcation. Let $(\alpha, \beta, h, m, c, \rho, k_0) \in \Omega_{NS}$, i.e., $k_0 = A_1 - A_4/A_1 A_4 - A_2 A_3$. Then, variation of $(\alpha, \beta, h, m, c, \rho, k)$ in small neighborhood of Ω_{NS} gives emergence to Neimark-Sacker bifurcation. Let K denote the perturbation parameter for the mapping (3), i.e., $|K|1$. The perturbed mapping is

$$\begin{pmatrix} x \\ y \end{pmatrix} \longrightarrow \begin{pmatrix} x + (k+K)x\left(1 - x - \dfrac{\alpha y}{m+x} - \dfrac{h}{c+x}\right) \\ y + (k+K)\rho y\left(1 - \dfrac{\beta y}{m+x}\right) \end{pmatrix}. \quad (41)$$

Define $X = x - \bar{x}$ and $Y = y - \bar{y}$, to translate the fixed point to $(0, 0)$. Here, $(\bar{x}, \bar{y})$ is the positive interior fixed point. Then, the above mapping is converted to
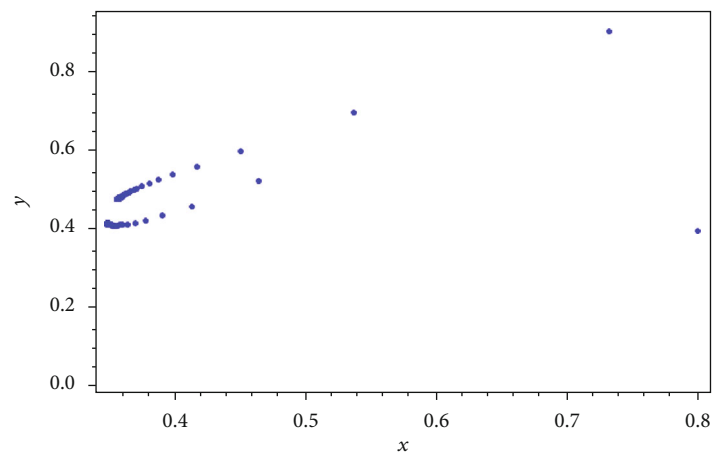
$$\begin{pmatrix} X \\ Y \end{pmatrix} \longrightarrow \begin{pmatrix} X + (k+K)(X+\bar{x})\left(1 - (X+\bar{x}) - \dfrac{\alpha(Y+\bar{y})}{m+(X+\bar{x})} - \dfrac{h}{c+(X+\bar{x})}\right) \\ Y + (k+K)\rho(Y+\bar{y})\left(1 - \dfrac{\beta(Y+\bar{y})}{m+(X+\bar{x})}\right) \end{pmatrix}. \quad (42)$$

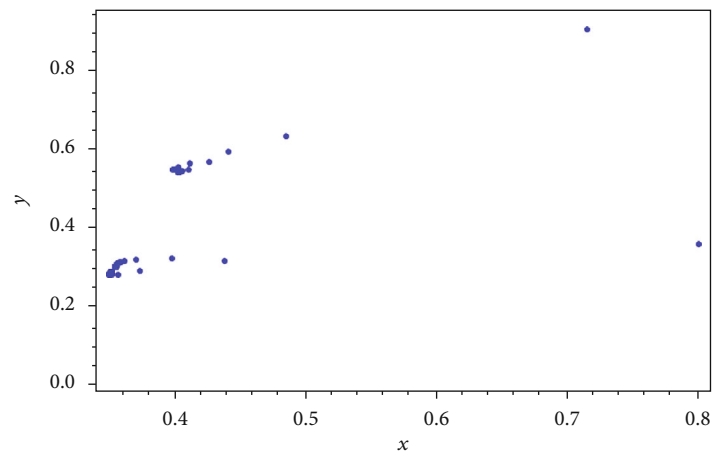After Taylor series expansion, the above mapping can be written as

$$\begin{pmatrix} X \\ Y \end{pmatrix} \longrightarrow \begin{pmatrix} c_{11} & c_{12} \\ c_{21} & c_{22} \end{pmatrix} \begin{pmatrix} X \\ Y \end{pmatrix} + \begin{pmatrix} f_{NS}(X, Y) \\ g_{NS}(X, Y) \end{pmatrix}, \quad (43)$$
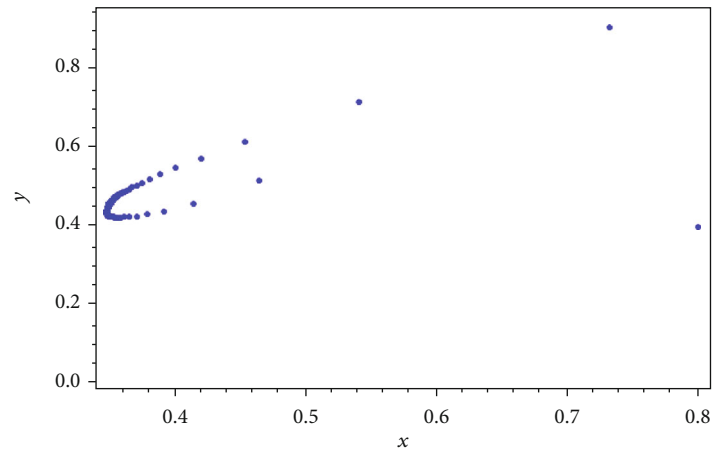
(a) $k = 0.88$

(b) $k = 0.89$
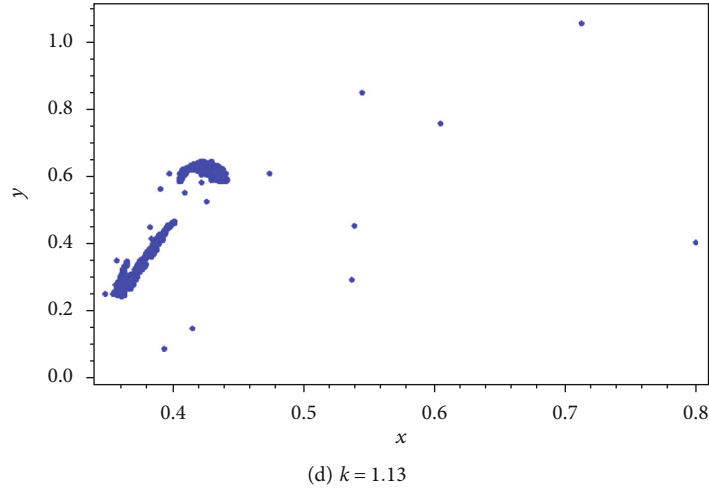

(c) $k = 1.06$

FIGURE 2: Continued.

(d) $k = 1.13$

FIGURE 2: Phase portraits for the system, with initial conditions $(x_0, y_0) = (0.8, 0.4)$, at parametric values $(\alpha, \beta, h, m, c, \rho) = (0.4, 1, 0.1, 0.1, 0.05, 2.6)$, around the bifurcation parameter $k_0 = 0.881137$.

where $c_{11} = 1 + (k + K)A_1$, $c_{12} = -(k + K)A_2$, $c_{21} = (k + K)A_3$, and $c_{22} = 1 - (k + K)A_4$, and

$$
\begin{aligned}
f_{NS}(X, Y) = {} & (k + K)b_1 X^2 + (k + K)b_2 XY + (k + K)b_3 Y^2 \\
& + kb_4 X^3 + kb_5 X^2 Y + kb_6 XY^2 \\
& + kb_7 Y^3 + O\left(|X + Y|^4\right),
\end{aligned}
$$

$$
\begin{aligned}
g_{NS}(X, Y) = {} & (k + K)b_8 X^2 + (k + K)b_9 XY + (k + K)b_{10} Y^2 \\
& + kb_{11} X^3 + kb_{12} X^2 Y + kb_{13} XY^2 \\
& + kb_{14} Y^3 + O\left(|X + Y|^4\right),
\end{aligned}
\tag{44}
$$

and b_i, $i \in \{1, 2, \cdots, 14\}$ are defined as above. Let the characteristic polynomial of matrix in (43) be

$$
p_{NS}(z) = z^2 - P(K)z + Q(K),
\tag{45}
$$

where

$$
\begin{aligned}
P(H) &= c_{11} + c_{22}, \\
Q(H) &= c_{11}c_{22} - c_{21}c_{12}.
\end{aligned}
\tag{46}
$$

Since $(\alpha, \beta, h, m, c, \rho, k) \in \Omega_{NS}$, therefore the roots of (45) are complex conjugate z_1, z_2, and $|z_1| = |z_2| = 1$, and it follows that $z_{1,2} = P(H)/2 \pm 1/2\sqrt{4Q(H) - P(H)^2}$ and $1 = |z_1| = |z_2| = \sqrt{Q(H)}$. Note that $P(K)^2 - 4Q(K) < 0$, which implies that $P(K)^2 < 4Q(K)$ or $P(K) \in (-2, 2)$. Also,

$$
\left(\frac{d|z_{1,2}|}{dK}\right)_{K=0} = \frac{1}{2}\left(\rho - \bar{x}\left(\frac{h}{(c + \bar{x})^2} + \frac{\alpha\bar{y}}{(m + \bar{x})^2} - 1\right)\right).
\tag{47}
$$

Thus, if $\rho \neq \bar{x}(h/(\bar{x} + c)^2 + \alpha\bar{y}/(\bar{x} + m)^2 - 1)$, then

$$
\left(\frac{d|z_{1,2}|}{dK}\right)_{K=0} \neq 0.
\tag{48}
$$

In order to ensure that the roots of the characteristic polynomial do not lie in the intersection of unit circle of coordinate axis when $K = 0$, we need to check that $z_{1,2}^m \neq 1$, for $m = 1, 2, 3, 4$ at $K = 0$. This is equivalent to checking $P(0) \neq -2, 0, 1, 2$. Since $(\alpha, \beta, h, m, c, \rho, k) \in \Omega_{NS}$, we already know that $P(0) \neq -2, 0, 2$. Finally,

$$
P(0) \neq 1 \Leftrightarrow k \neq \frac{1}{A_4 - A_1}.
\tag{49}
$$

Thus, the roots of (45) do not lie in the intersection of unit circle of coordinate axis when $K = 0$. Now, to convert the system (43) to the normal form, when $K = 0$, let $R = P(0)/2$ and $S = 1/2\sqrt{4Q(0) - P(0)^2}$ and let

$$
T_{NS} = \begin{pmatrix} 0 & 1 \\ S & R \end{pmatrix}.
\tag{50}
$$

Here, T_{NS} is an invertible matrix. Consider the transformation

$$
\begin{pmatrix} X \\ Y \end{pmatrix} = T_{NS} \begin{pmatrix} u \\ v \end{pmatrix}.
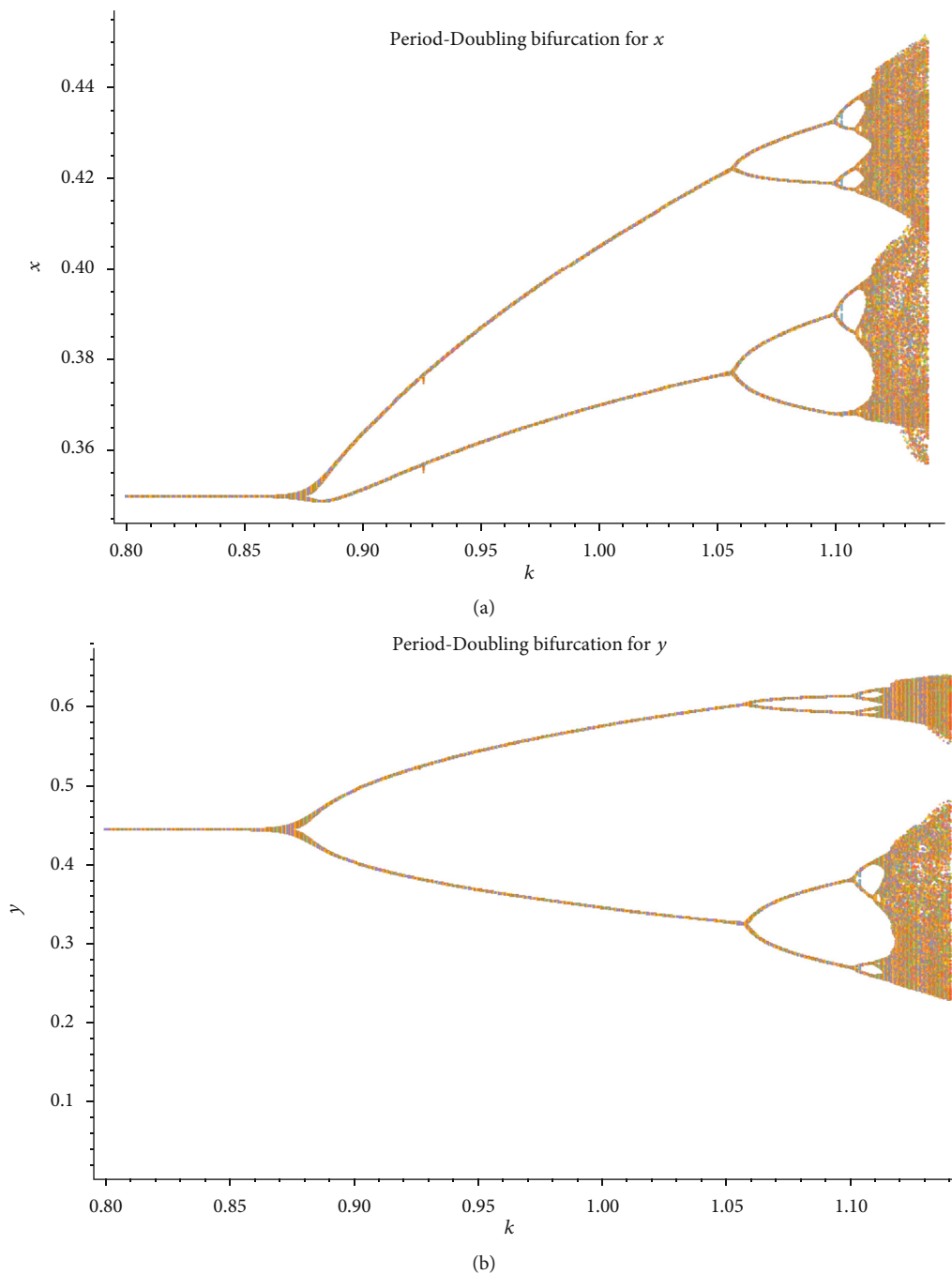\tag{51}
$$

(a)

(b)

FIGURE 3: Period-Doubling bifurcation diagrams for positive interior points of the model (3), in the interval $k \in [0.8, 1.14]$, with initial conditions $(x_0, y_0) = (0.8, 0.4)$ and the parametric values $(\alpha, \beta, h, m, c, \rho) = (0.4, 1, 0.1, 0.1, 0.05, 2.6)$.

The system (43) can be written as

$$\begin{pmatrix} u \\ v \end{pmatrix} \longrightarrow \begin{pmatrix} R & -S \\ S & R \end{pmatrix} \begin{pmatrix} u \\ v \end{pmatrix} + \begin{pmatrix} \tilde{f}_{NS}(u, v) \\ \tilde{g}_{NS}(u, v) \end{pmatrix}, \qquad (52)$$

where

$$\tilde{f}_{NS}(u, v) = e_1 u^2 + e_2 uv + e_3 v^2 + e_4 u^3 + e_5 u^2 v + e_6 uv^2 + e_7 v^3 + O(|u + v|^4),$$

$$\tilde{g}_{NS}(u, v) = e_8 u^2 + e_8 uv + e_{10} v^2 + e_{11} u^3 + e_{12} u^2 v + e_{13} uv^2 + e_{14} v^3 + O(|u + v|^4), \qquad (53)$$

and

$$e_1 = \frac{(k + K)(-R(b_2 S + b_1) + S(b_{10} S + b_9) + b_8)}{S},$$
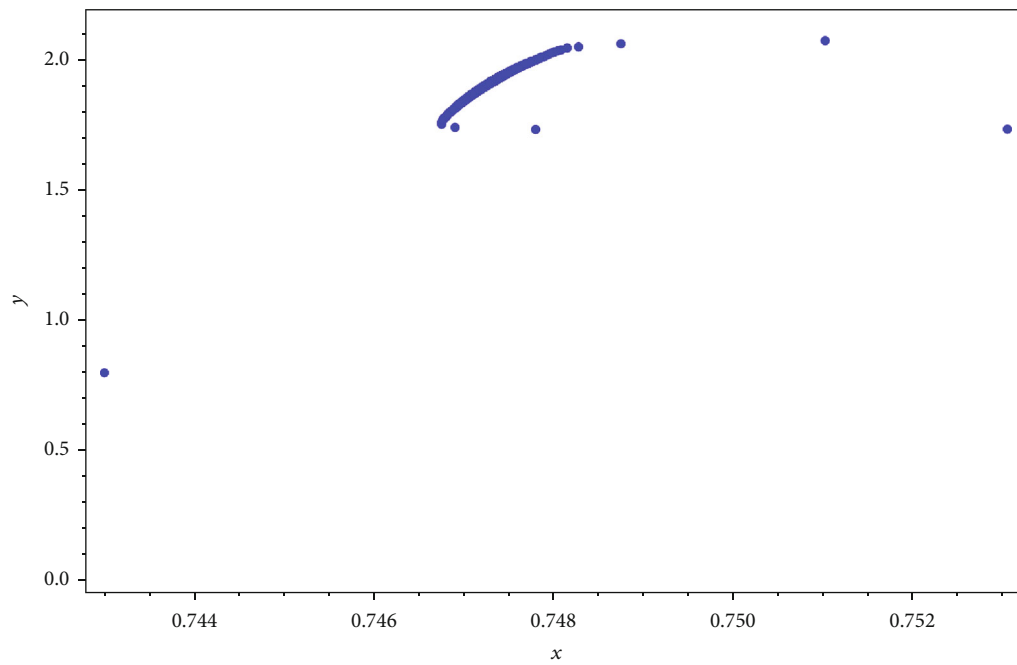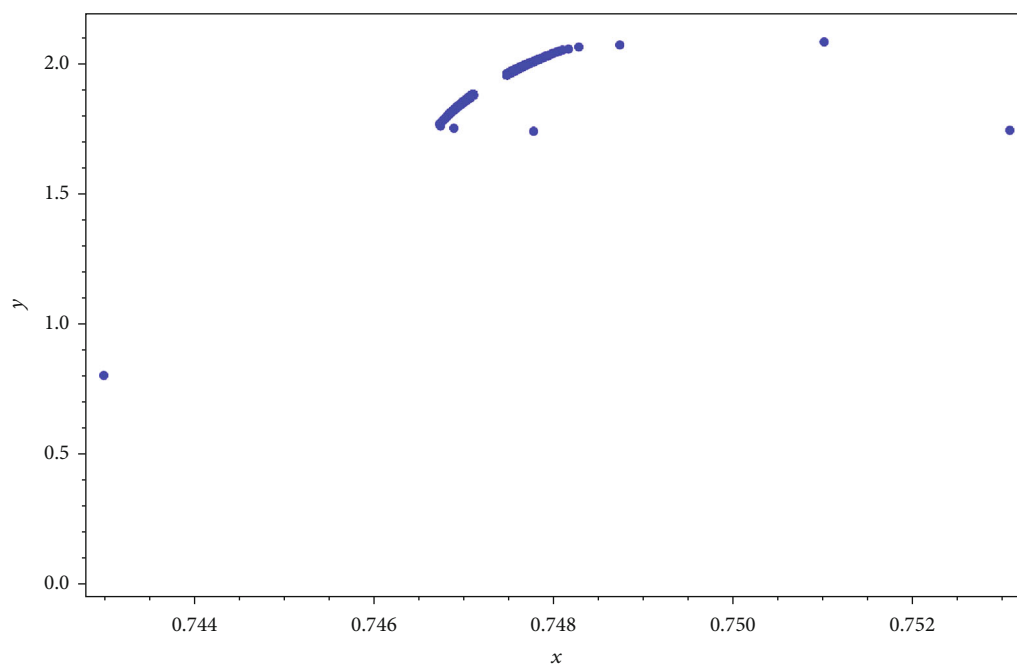
$$e_2 = \frac{(b_2(-R) + 2b_{10} S + b_9)(R(k + K))}{S},$$

(a) $k = 1.06$

(b) $k = 1.062$

Figure 4: Continued.

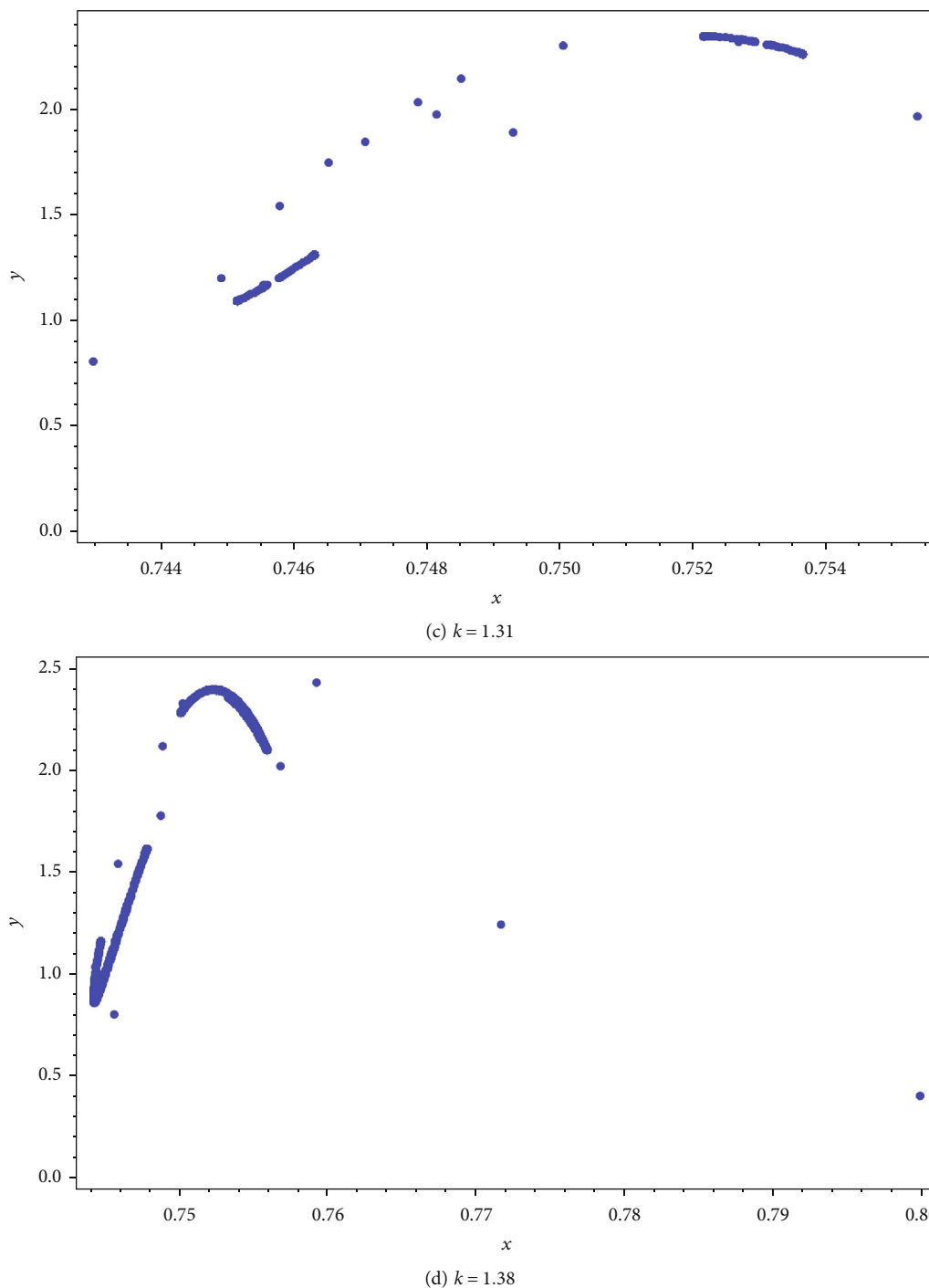(c) $k = 1.31$

(d) $k = 1.38$

FIGURE 4: Phase portraits for the system, with initial conditions $(x_0, y_0) = (0.3, 0.6)$, at parametric values $(\alpha, \beta, h, m, c, \rho) = (0.01, 0.6, 0.2, 0.4, 0.1, 1.9)$, around the bifurcation parameter $k_0 = 1.06112$.

$$e_4 = \frac{k(-R(b_5 S + b_4) + S(b_{13} S + b_{12}) + b_{11})}{S},$$

$$e_3 = \frac{b_{10}(R^2(k + K))}{S},$$

$$e_5 = \frac{(kR)((2b_{13}S + b_{12}) - b_5 R)}{S},$$

$$e_6 = \frac{b_{13}(kR^2)}{S},$$

$$e_7 = 0,$$

$$e_8 = (b_2 S + b_1)(k + K),$$

$$e_9 = b_2 R(k + K),$$

Period-Doubling bifurcation for x

(a)

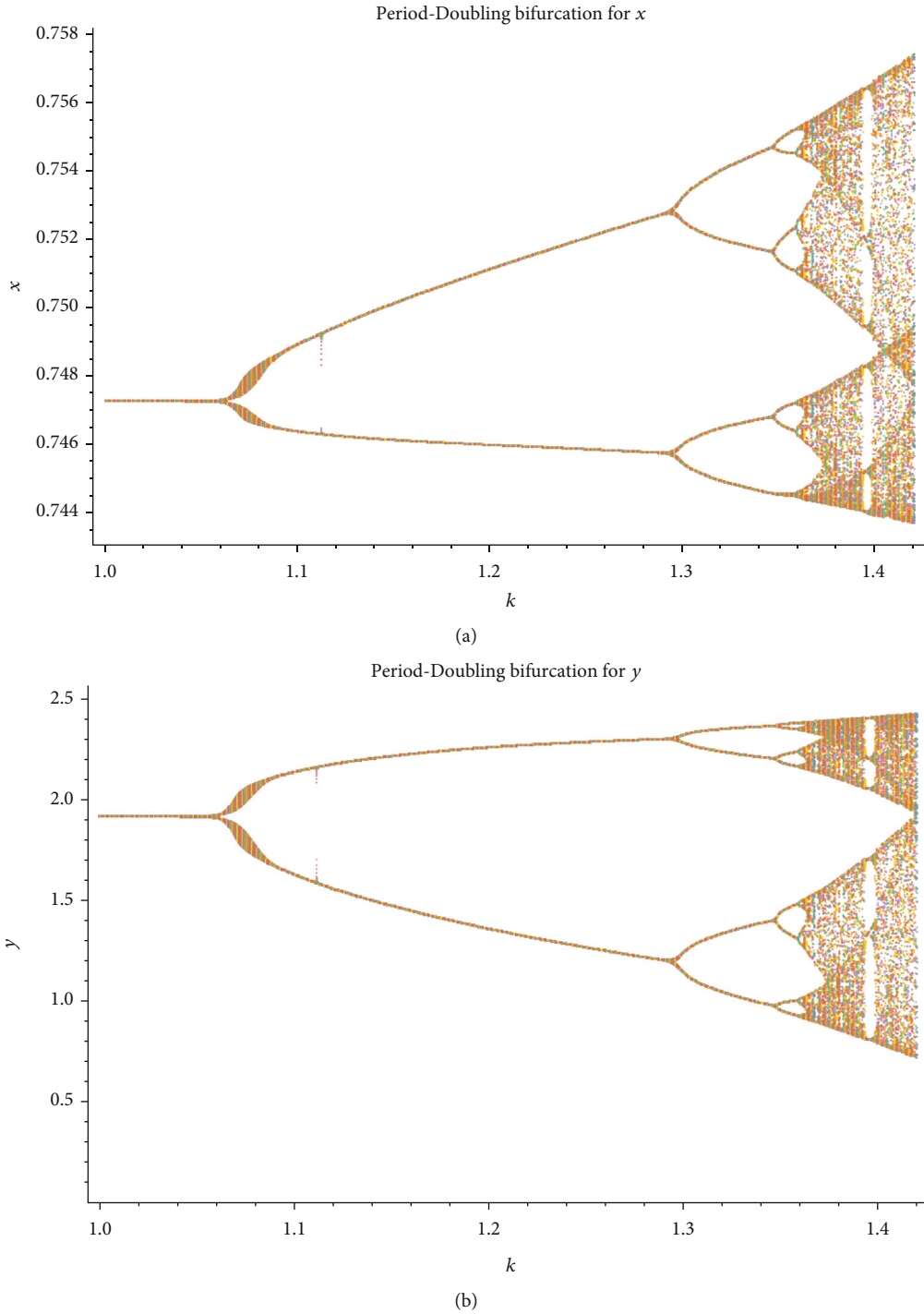Period-Doubling bifurcation for y

(b)

FIGURE 5: Period-doubling bifurcation diagrams for positive interior points of the model (3), in the interval $k \in [1, 1.42]$, with initial conditions $(x_0, y_0) = (0.3, 0.6)$ and the parametric values $(\alpha, \beta, h, m, c, \rho) = (0.01, 0.6, 0.2, 0.4, 0.1, 1.9)$.

$$e_{10} = 0,$$
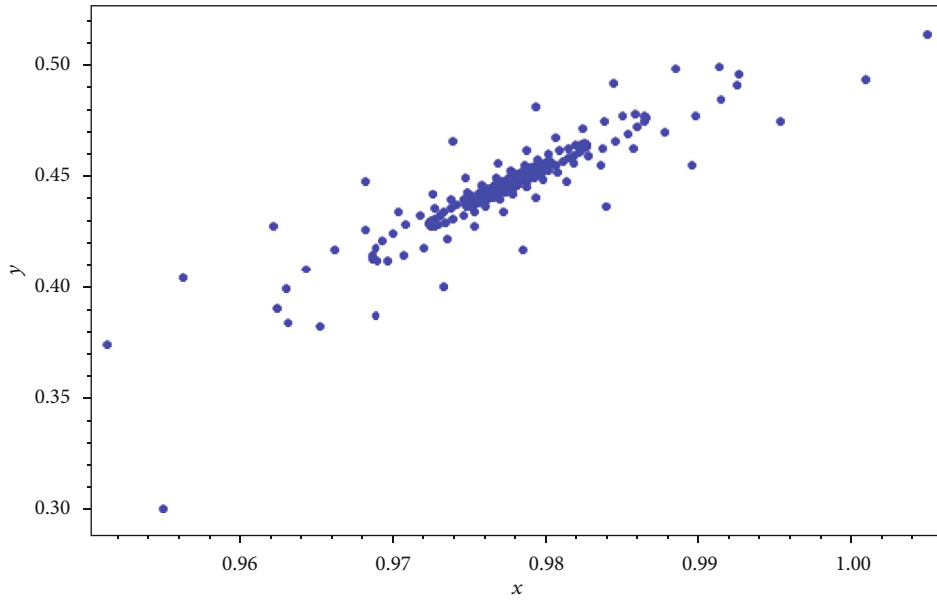
$$e_{11} = k(b_5 S + b_4),$$

$$e_{12} = b_5 kR,$$
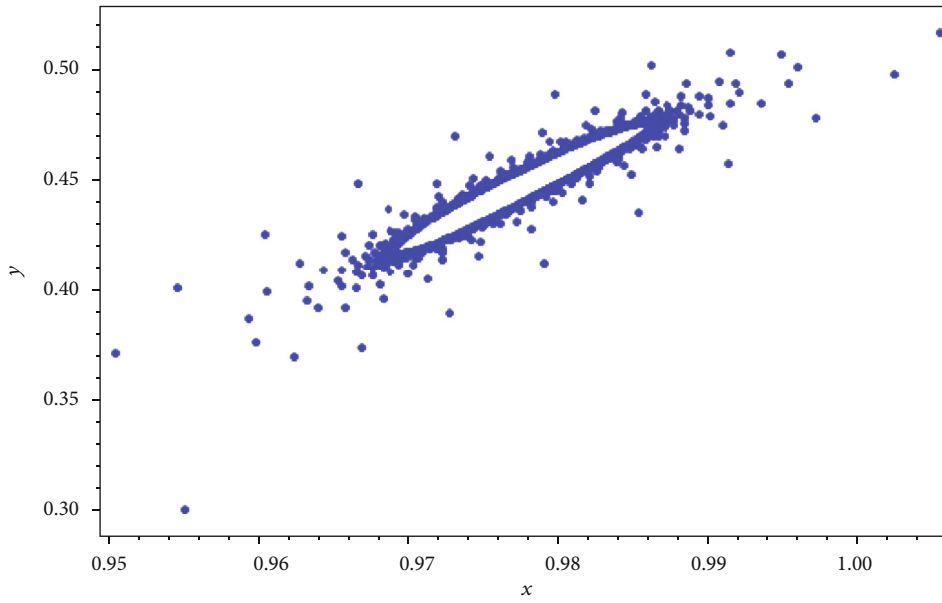
$$e_{13} = 0,$$

$$e_{14} = 0, X = v, Y = Su + Rv. \tag{54}$$

For the map (52) to undergo Neimark-Sacker bifurcation, the following quantity must not zero [22]:

$$M_{NS} = \left(\left[-\mathrm{Re}\left(\omega_{20}\omega_{11} \frac{(1 - 2z_1)z_2^2}{1 - z_1} \right) - \frac{1}{2}|\omega_{11}|^2 - |\omega_{02}|^2 + \mathrm{Re}\,(\omega_{21}z_2) \right] \right)_{K=0}, \tag{55}$$
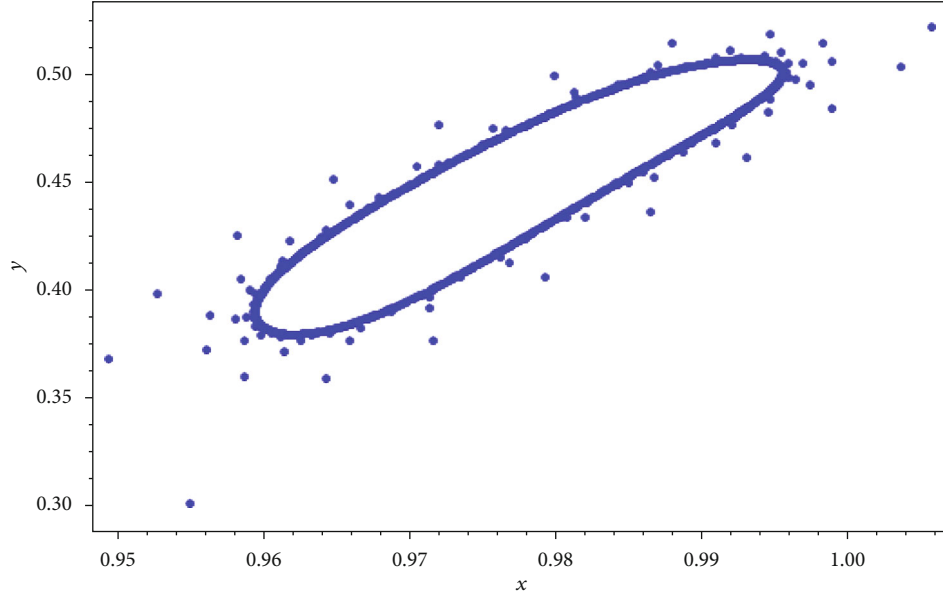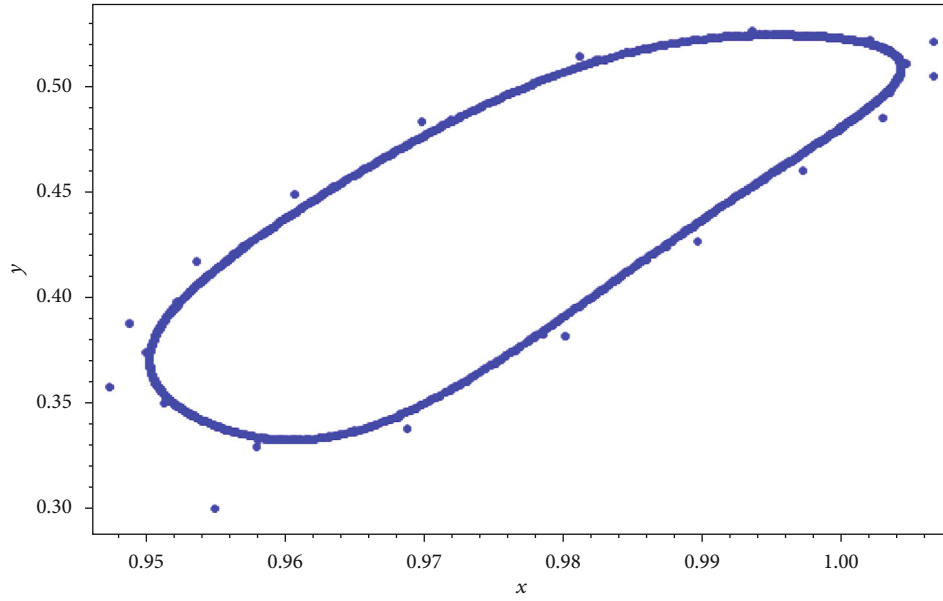
(a) A stable spiral point at $k = 1.78$

(b) An invariant closed curve at $k = 1.795$

FIGURE 6: Continued.

(c) Larger attracting invariant closed curves with some rough edges at $k = 1.81$

(d) Larger attracting invariant closed curves with edges starting to vanish at $k = 1.84$

FIGURE 6: Phase portraits for the parametric values $(\alpha, \beta, h, m, c, \rho, k_0) = (0.05, 2.3, 0.001, 0.05, 0.5, 1.275, 1.79111)$ at $(\bar{x}, \bar{y}) = (0.977584, 0.446776)$.
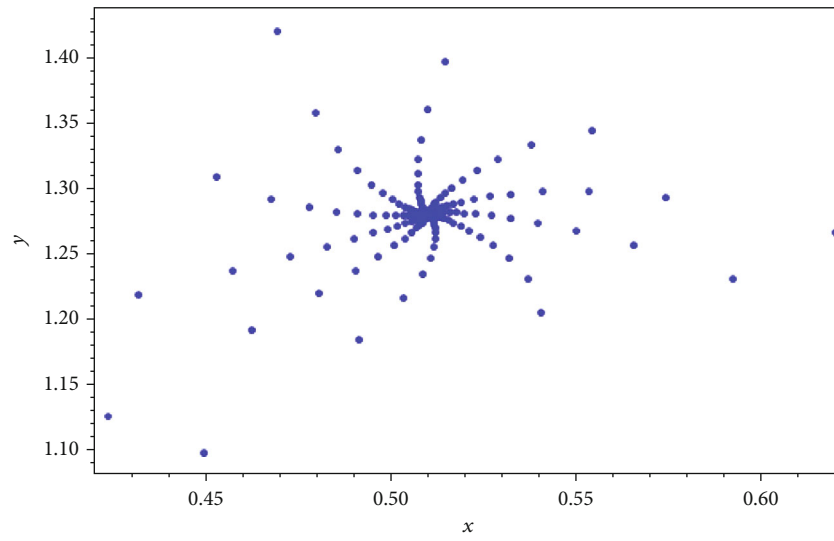
where

$$\omega_{20} = \frac{1}{8}\left[\frac{\partial^2 \bar{f}_{NS}}{\partial u^2} - \frac{\partial^2 \bar{f}_{NS}}{\partial v^2} + 2\frac{\partial^2 \bar{g}_{NS}}{\partial u \partial v}\right. \\ \left. + \iota\left(\frac{\partial^2 \bar{g}_{NS}}{\partial u^2} - \frac{\partial^2 \bar{g}_{NS}}{\partial v^2} - 2\frac{\partial^2 \bar{f}_{NS}}{\partial u \partial v}\right)\right],$$
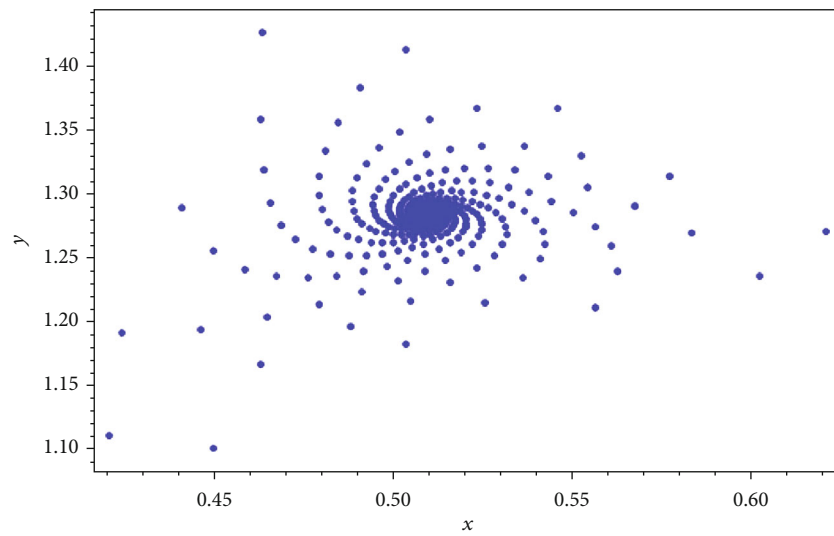
$$\omega_{11} = \frac{1}{4}\left[\frac{\partial^2 \bar{f}_{NS}}{\partial u^2} + \frac{\partial^2 \bar{f}_{NS}}{\partial v^2} + \iota\left(\frac{\partial^2 \bar{g}_{NS}}{\partial u^2} + \frac{\partial^2 \bar{g}_{NS}}{\partial v^2}\right)\right],$$

$$\omega_{02} = \frac{1}{8}\left[\frac{\partial^2 \bar{f}_{NS}}{\partial u^2} - \frac{\partial^2 \bar{f}_{NS}}{\partial v^2} - 2\frac{\partial^2 \bar{g}_{NS}}{\partial u \partial v}\right. \\ \left. + \iota\left(\frac{\partial^2 \bar{g}_{NS}}{\partial u^2} - \frac{\partial^2 \bar{g}_{NS}}{\partial v^2} + 2\frac{\partial^2 \bar{f}_{NS}}{\partial u \partial v}\right)\right],$$

$$\omega_{21} = \frac{1}{16}\left[\frac{\partial^3 \bar{f}_{NS}}{\partial u^3} + \frac{\partial^3 \bar{f}_{NS}}{\partial u \partial v^2} + \frac{\partial^3 \bar{g}_{NS}}{\partial u^2 \partial v} + \frac{\partial^3 \bar{g}_{NS}}{\partial v^3}\right. \\ \left. + \iota\left(\frac{\partial^3 \bar{g}_{NS}}{\partial u^3} + \frac{\partial^3 \bar{g}_{NS}}{\partial u \partial v^2} - \frac{\partial^3 \bar{f}_{NS}}{\partial u^2 \partial v} - \frac{\partial^3 \bar{f}_{NS}}{\partial v^3}\right)\right].$$
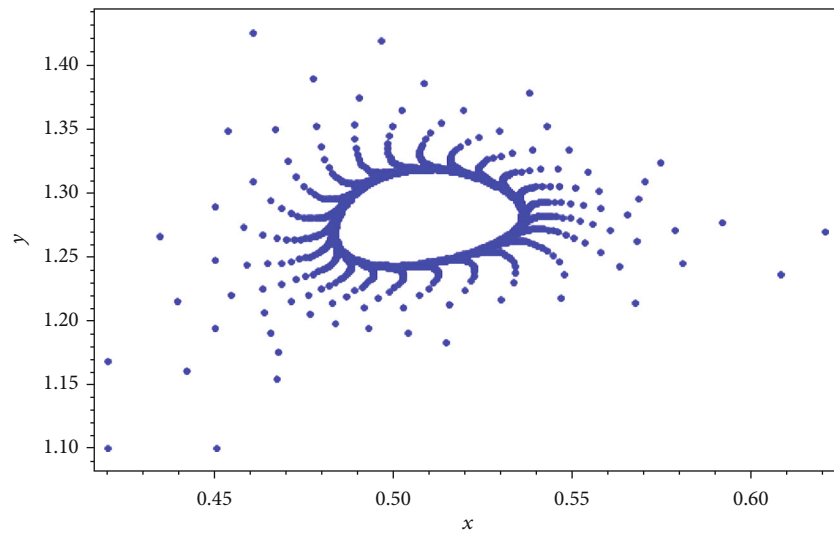
(56)

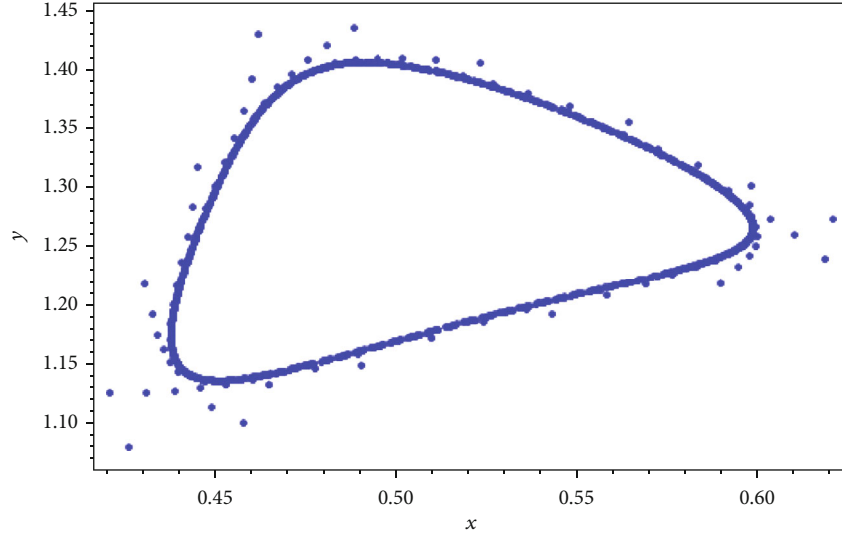(a) A small stable spiral at $k = 3.66$

(b) A large stable spiral at $k = 3.71$

(c) An invariant closed curve with many edges at $k = 3.74$

FIGURE 7: Continued.

(d) Larger attracting invariant closed curves with edges starting to vanish at $k = 3.79$

FIGURE 7: Phase portraits for model (3) for the parametric values at $(\bar{x}, \bar{y}) = (0.50972255689403, 1.2815659608127545)$.

Using the result in [57] and the above analysis, we have the following result.

Theorem 7. *If $k \neq 1/A_4 - A_1$ and M_{NS} defined in (55) is nonzero, then the model (5) undergoes Neimark-Sacker bifurcation at the equilibrium point $(\bar{x}, \bar{y})$, provided that parameter k changes in the small neighborhood of $k_0 = A_1 - A_4/A_1A_4 - A_2A_3$ and $(\alpha, \beta, h, m, c, \rho, k_0) \in \Omega_{NS}$. Moreover, if $M_{NS} < 0$ (resp., $M_{NS} > 0$), then an attracting (resp., repelling) invariant closed curve bifurcate from the fixed point $(\bar{x}, \bar{y})$ for $k > k_0$ (resp., $k < k_0$).*

5. Numerical Simulations

In this section, we will present some examples which will show the presence of period-doubling and Neimark-Sacker bifurcations for the system (3), using specific numerical values of its parameters $(\alpha, \beta, h, m, c, \rho)$ and taking the step-size, k, as the bifurcation parameter. The illustration will be done using bifurcation diagrams, and it will be ratified by showing that Theorems 5 and 7 are satisfied.

Example 1. Select $(\alpha, \beta, h, m, c, \rho) = (0.4, 1, 0.1, 0.1, 0.05, 2.6)$, $k \in [0.8, 1.14]$, and the initial value $(x_0, y_0) = (0.8, 0.4)$. The Jacobian matrix is

$$\begin{pmatrix} 1 + 0.179861k & -0.311111k \\ 2.6k & 1 - 2.6k \end{pmatrix}, \qquad (57)$$

and $z_1 = 1 - 2.26979k$ and $z_2 = 1 - 0.150344k$ are the corresponding eigenvalues. Both eigenvalues are less then 1, for any $k > 0$. Also, $z_1 = -1$ and $z_2 \in (-1, 1)$, if $k = 0.881137$ and $z_1 < -1$ and $z_2 = -1$, if $k = 13.3028$. Thus, with these parametric conditions, the fixed point is never unstable or saddle. The fixed point is stable for any $k \neq 0.881137$, or $k = 13.3028$; otherwise, the fixed point undergoes period-

doubling bifurcation, as k varies in the small neighborhood of k_0, where let $k_0 = 0.881137$. From the phase portrait in Figure 2(b), it is apparent that the fixed point $(0.35, 0.45)$ of map (3) is stable for $k < 0.881137$ and the period-doubling bifurcation occurs around 0.881137. Figure 2(c) shows that another stable period-doubling bifurcation at around $k = 1.06$. This can also be verified using the bifurcation diagrams in Figure 3.

After calculations, we get, $Y_1 = 0.330205 \neq 0$ and $Y_2 = 336.675 \neq 0$. These values further complement the dynamics of our map, observed above and proves the correctness of Theorem 5. Moreover, $Y_2 > 0$, which shows that the period-two orbits that bifurcate from positive equilibrium are stable.

Example 2. Select $(\alpha, \beta, h, m, c, \rho) = (0.01, 0.6, 0.2, 0.4, 0.1, 1.9)$, $k \in [1, 1.42]$, and the initial value $(x_0, y_0) = (0.3, 0.6)$. The Jacobian matrix is

$$\begin{pmatrix} 1 - 0.528241k & -0.00651351k \\ 3.16667k & 1 - 1.9k \end{pmatrix}, \qquad (58)$$

and $z_1 = 1 - 1.8848k$ and $z_2 = 1 - 0.543446k$ are the corresponding eigenvalues. Both eigenvalues are less then 1, for any $k > 0$. Also, $z_1 = -1$ and $z_2 \in (-1, 1)$, if $k = 1.06112$ and $z_1 < -1$ and $z_2 = -1$, if $k = 3.68022$. Thus, with these parametric conditions, the fixed point is never unstable or saddle. The fixed point is stable for any $k \neq 1.06112$, or $k = 3.68022$; otherwise, the fixed point undergoes period-doubling bifurcation, as k varies in the small neighborhood of k_0, where let $k_0 = 1.06112$. From the phase portrait in Figure 4(b), it is apparent that the fixed point $(0.747285, 1.91214)$ of map (3) is stable for $k < 1.06112$ and the period-doubling bifurcation occurs around 1.06112. Figure 4(c) shows that another stable period-doubling bifurcation at around $k = 1.31$. This can also be verified using the bifurcation diagrams in Figure 5.

Neimarck-Sacker Bifurcation for x

(a)

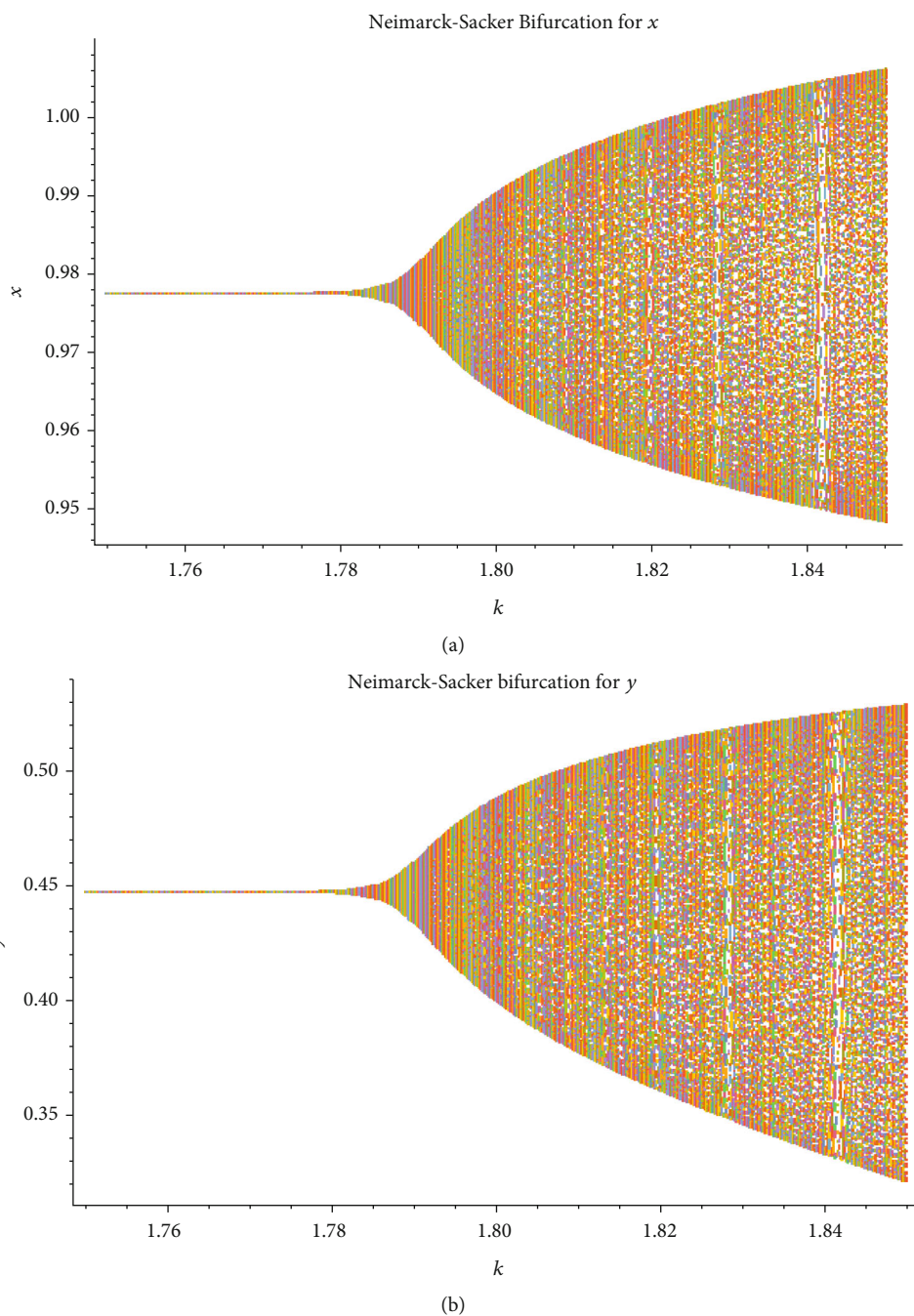Neimarck-Sacker bifurcation for y

(b)

FIGURE 8: Bifurcation diagrams for initial conditions $(x_0, y_0) = (0.955, 0.3)$ and $k \in [1.75, 1.85]$, with parameters $(\alpha, \beta, h, m, c, \rho) = (0.05, 2.3, 0.001, 0.05, 0.5, 1.275)$, at $(\bar{x}, \bar{y}) = (0.977584, 0.446776)$.

After calculations, we get, $Y_1 = -0.23876 \neq 0$ and $Y_2 = 8.71736 \neq 0$. These values further complement the dynamics of our map, observed above and proved the correctness of Theorem 5. Moreover, $Y_2 > 0$, which shows that the period-two orbits that bifurcate from positive equilibrium are stable.

5.1. Neimark-Sacker Bifurcation

Example 3. Let us assume the following parameter values, $(\alpha, \beta, h, m, c, \rho) = (0.05, 2.3, 0.001, 0.05, 0.5, 1.275)$, $k \in [1.75, 1.85]$,

and the initial value $(x_0, y_0) = (0.955, 0.3)$. The Jacobian matrix is

$$\begin{pmatrix} 1 - 0.956455k & -0.0475671k \\ 0.554348k & 1 - 1.275k \end{pmatrix}, \qquad (59)$$

and $z_1 = -0.998393 - 0.056668\iota$ and $z_2 = -0.998393 + 0.056668\iota$ are the corresponding eigenvalues, for $k = k_0 = 1.79111$. Both eigenvalues are on the unit circle. Also,

Neimarck-Sacker bifurcation for x

(a)

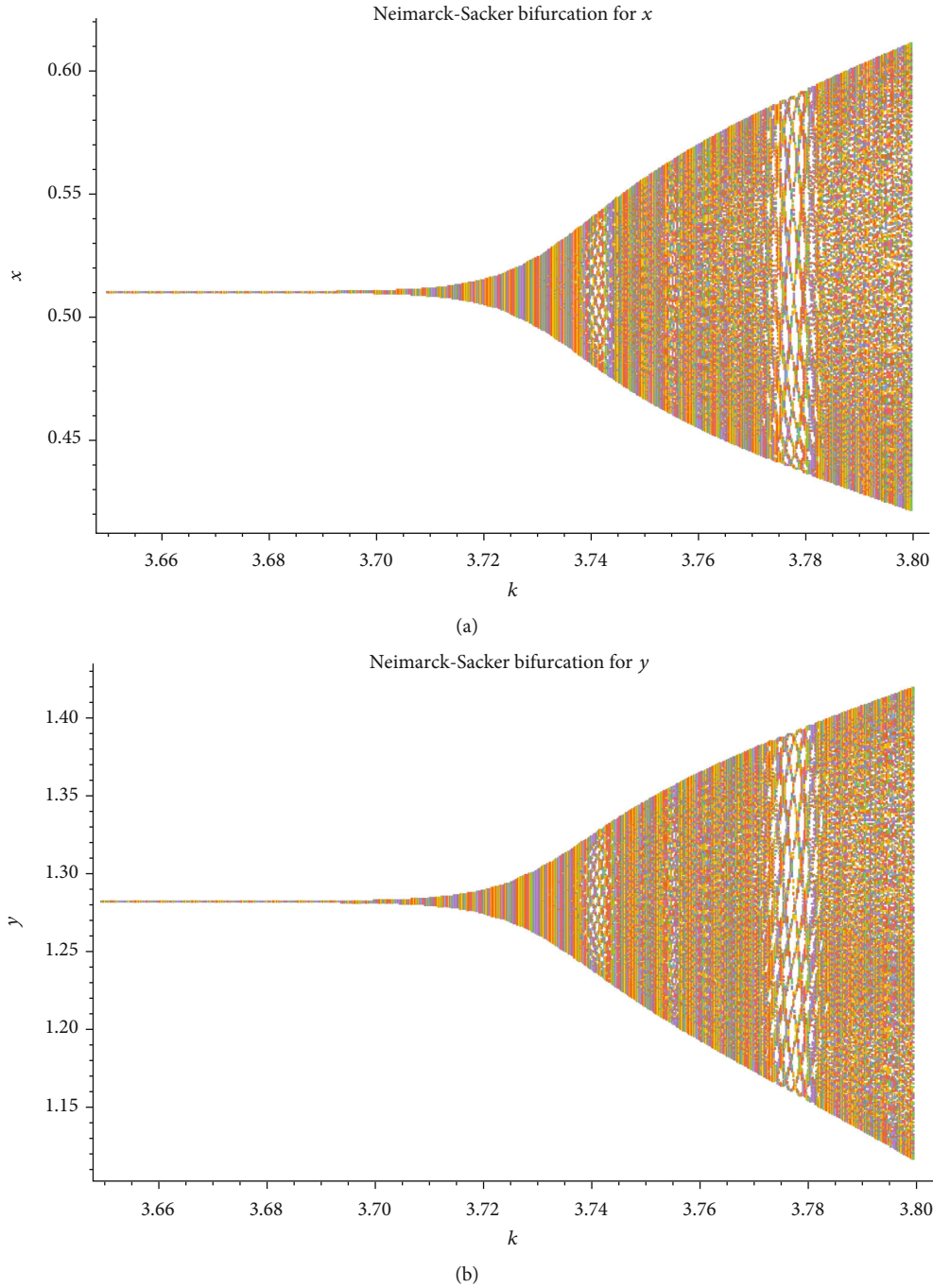Neimarck-Sacker bifurcation for y

(b)

FIGURE 9: Bifurcation diagrams for initial conditions $(x_0, y_0) = (0.45, 1.1)$ and $k \in [3.71, 3.85]$, at $(\bar{x}, \bar{y}) = (0.50972255689403, 1.2815659608127545)$, with parameters $(\alpha, \beta, h, m, c, \rho) = (0.5, 1.1, 0.02, 0.9, 0.05, 0.4)$.

$k_0 \neq 1/A_4 - A_1 = 0.448138$, $k_0 \in (0, 4/A_4 - A_1) = (0, 1.79255)$, $(d|z_1|/dK)_{K=0} = (d|z_2|/dK)_{K=0} = 1.11573 \neq 0$ and $M_{NS} = -1297652.848483635 \neq 0$. Thus, the fixed point exhibits Neimark-Sacker bifurcation, at the fixed point $(\bar{x}, \bar{y}) = (0.977584, 0.446776)$. Moreover, since $M_{NS} < 0$, an attracting invariant closed curve bifurcates from the fixed point $(0.977584, 0.446776)$ for $k > 1.79111$.

From the phase portrait in Figure 6(a), the attractor becomes a stable spiral point and as the parameter k increases, and the stable spiral enlarges in size. As k continues to increase, the spiral becomes larger before changing in to an attracting invariant closed curve with rough edges due to Neimark-Sacker bifurcation. This spiral and edges are plotted in Figure 6(b) at $k = 1.795$. At $k = 1.81$, the attracting invariant closed curves become larger with some rough edges as shown in Figure 6(c). It is clear from the close values of the parameter k how quasi-periodic motions are produced around fixed point due to this type of bifurcation. Increasing k furthermore gives rise to continued invariant closed curves

around the fixed point, but their edges begin to vanish as plotted in Figure 6(d).

Example 11. Let us assume that for $k \in [3.71,3.85]$ and the initial value $(x_0, y_0) = (0.45,1.1)$, we have the following parameter values, $(\alpha, \beta, h, m, c, \rho) = (0.5,1.1,0.02,0.9,0.05,0.4)$. The Jacobian matrix is

$$\begin{pmatrix} 1 - 0.31283k & -0.180788k \\ 0.363636k & 1 - 0.4k \end{pmatrix}, \qquad (60)$$

and $z_1 = -0.331058 - 0.943611\iota$ and $z_2 = -0.331058 + 0.943611\iota$ are the corresponding eigenvalues, for $k = k_0 = 3.734575030140114$. Both eigenvalues are on the unit circle. Also, $k_0 \neq 1/A_4 - A_1 = 1.40286$, $k_0 \in (0, 4/A_4 - A_1) = (0,5.61144)$, $(d|z_1|/dK)_{K=0} = (d|z_2|/dK)_{K=0} = 0.356415 \neq 0$, and $M_{NS} = -6.56955 \neq 0$. Thus, the fixed point exhibits Neimark-Sacker bifurcation, at the equilibrium point $(\bar{x}, \bar{y}) = (0.50972255689403,1.2815659608127545)$. Moreover, since $M_{NS} < 0$, an attracting invariant closed curve bifurcates from the fixed point for $k > 3.734575030140114$.

From the phase portrait in Figure 7(a), we can see that the attractor becomes a stable spiral point and as the parameter k increases, the stable spiral enlarges in size (Figure 7(b)). As k continues to increase, the spiral becomes larger before changing into an attracting invariant closed curve with rough edges due to Neimark-Sacker bifurcation. This spiral and edges are plotted in Figure 7(c) at $k = 3.74$. At $k = 3.79$, we see continued invariant closed curves around the fixed point, but their edges begin to vanish as plotted in Figure 7(d).

6. Conclusion

In this paper, we studied the existence and stability of the positive interior fixed points of system (5) and flip bifurcation and Neimark-Sacker bifurcation, under certain conditions, by using central manifold theorem and bifurcation theory. Our main results are given in Theorem 3 and Theorems 5 and 7 and numerical simulations in Section 5. In the details of the result, when the integral step size k is chosen as a bifurcation parameter, the discrete-time modified Leslie-Gower system with Michaelis-Menten-type prey harvesting displays much richer dynamical behavior. It can be seen from Figures 3–9 that the system displays period-1, 2, 4, and 8 orbits. Moreover, Figures 3 and 5 show that the system exhibits period-doubling bifurcation, and the period-two orbits that bifurcate from positive equilibrium are stable, which shows the correctness of Theorem 5. Similarly, Figures 8 and 9 show that the system exhibits Neimark-Sacker bifurcation, with an attracting invariant closed curve bifurcates from the fixed point, proving the correctness of Theorem 7.

Data Availability

All data required for this paper is included within this paper.

Conflicts of Interest

The authors do not have any competing interests.

Authors' Contributions

Hengxiao Qi analyzed the results and wrote the final version of this paper, M. Saqib Khan proved the main results. Mujahid Abbas proposed the problem and supervised this work. and Ebenezer Bonyah wrote the first version of this paper.

Acknowledgments

References

[1] S. Allesina and S. Tang, "Stability criteria for complex ecosystems," *Nature*, vol. 483, no. 7388, pp. 205–208, 2012.

[2] C. W. Clark, *Mathmatics Bioeconomics, The Optimal Management of Renewable Re-sources*, John Wiley & Sons, Inc, New York-London-Sydney, 1976.

[3] A. J. Lotka, "Analytical note on certain rhythmic relations in organic systems," *Proceedings of the National Academy of Sciences of the United States of America*, vol. 6, no. 7, pp. 410–415, 1920.

[4] V. Volterra, "Variations and fluctuations of the number of individuals in animal species living together," in *Animal Ecology*, R. N. Chapman, Ed., pp. 409–448, McGraw-Hill, New York, NY, USA, 1931.

[5] C. S. Holling, "The functional response of predators to prey density and its role in mimicry and population regulation," *Memoirs of the Entomological Society of Canada*, vol. 97, no. S45, pp. 5–60, 1965.

[6] P. H. Leslie, "A stochastic model for studying the properties of certain biological systems by numerical methods," *Biometrika*, vol. 45, no. 1-2, pp. 16–31, 1958.

[7] S. B. Hsu and T. W. Huang, "Global stability for a class of predator-prey system," *SIAM Journal on Applied Mathematics*, vol. 55, no. 3, pp. 763–783, 1995.

[8] R. M. May, *Stability and Complexity in Model Ecosystems*, Princeton University Press, Princeton, NJ, USA, 1973.

[9] L. Chen and F. Chen, "Global stability of a Leslie-Gower predator-prey model with feedback controls," *Applied Mathematics Letters*, vol. 22, no. 9, pp. 1330–1334, 2009.

[10] S. B. Hsu and T. W. Hwang, "Uniqueness of limit cycles for a predatorprey system of Holling and Lesile type," *Canadian Applied Mathematics Quarterly*, vol. 6, pp. 91–117, 1998.

[11] S. B. Hsu and T. W. Hwang, "Hopf bifurcation analysis for a predatorprey system of Holling and Leslie type," *Taiwanese Journal of Mathematics*, vol. 3, pp. 35–53, 1999.

[12] J. Huang, S. Ruan, and J. Song, "Bifurcations in a predator-prey system of Leslie type with generalized Holling type III functional response," *Journal of Differential Equations*, vol. 257, no. 6, pp. 1721–1752, 2014.

[13] M. A. Aziz-Alaoui and O. M. Daher, "Boundedness and globalstability for a predator-prey model with modified Leslie-Gower and Holling-type II schemes," *Applied Mathematics Letters*, vol. 16, no. 7, pp. 1069–1075, 2003.

[14] G. Caughley, "Plant-herbivoresystems," in *Theoretical Ecology: Principles and Applications*, R. M. May, Ed., pp. 94–113, W. B. Saunders Co, Philadelphia, PA, 1976.

[15] D. J. Wollkind and J. A. Logan, "Temperature-dependent predator-prey mite ecosystem on apple tree foliage," *Journal of Mathematical Biology*, vol. 6, no. 3, pp. 265–283, 1978.

[16] D. J. Wollkind, J. B. Collings, and J. A. Logan, "Metastability in a temperature-dependent model system for predator-prey mite outbreak interactions on fruit trees," *Journal of Mathematical Biology*, vol. 50, no. 4, pp. 379–409, 1988.

[17] Y. Liu and Z. Zeng, "Analysis of a predator-prey model with Crowley-Martin and modified Leslie-Gower schemes with stochastic perturbation," *Journal of Applied Analysis & Computation*, vol. 9, no. 6, pp. 2409–2435, 2019.

[18] M. Bilal Ajaz, U. Saeed, Q. Din, I. Ali, and M. Israr Siddiqui, "Bifurcation analysis and chaos control in discrete-time modified Leslie-Gower prey harvesting model," *Advances in Difference Equations*, vol. 2020, no. 1, 2020.

[19] Z. K. Guo, H. F. Huo, Q. Y. Ren, and H. Xiang, "Bifurcation of a modified Leslie-Gower system with discrete and distributed delays," *Journal of Nonlinear Modeling and Analysis*, vol. 1, no. 1, pp. 73–91, 2019.

[20] C. Y. Ji, D. Q. Jiang, and N. Z. Shi, "Analysis of a predator-prey model with modified Leslie-Gower and Holling-type II schemes with stochastic perturbation," *Journal of Mathematical Analysis and Applications*, vol. 359, no. 2, pp. 482–498, 2009.

[21] M. Liu, C. X. Du, and M. L. Deng, "Persistence and extinction of a modified Leslie-Gower Holling-type II stochastic predator-prey model with impulsive toxicant input in polluted environments," *Nonlinear Analysis: Hybrid Systems*, vol. 27, pp. 177–190, 2018.

[22] X. Y. Song and Y. F. Li, "Dynamic behaviors of the periodic predator-prey model with modified Leslie-Gower Holling-type II schemes and impulsive effect," *Nonlinear Analysis: Real World Applications*, vol. 9, no. 1, pp. 64–79, 2008.

[23] J. Jiang and Y. Song, "Stability and bifurcation analysis of a delayed Leslie-Gower predator-prey system with nonmonotonic functional response," *Abstract and Applied Analysis*, vol. 2013, Article ID 152459, 19 pages, 2013.

[24] J. M. Drake and A. M. Kramer, "Allee effects," *Nature Education Knowledge*, vol. 3, no. 10, p. 2, 2011.

[25] F. Courchamp, L. Berec, and J. Gascoigne, *Allee Effects in Ecology and Conservation*, Oxford University Press, Oxford New York, 2008.

[26] E. Gonzlez-Olivares, B. Gonzlez-Yaez, J. Mena-Lorca, and R. Ramos-Jiliberto, "Modelling the Allee effect: are the different mathematical forms proposed equivalents?," in *Proceedings of the 2006 international symposium on mathematical and computational biology BIOMAT*, vol. 2007, pp. 53–71, Manaus, Brazil, 2006.

[27] A. Kent, C. P. Doncaster, and T. Sluckin, "Consequences for predators of rescue and Allee effects on prey," *Ecological Modelling*, vol. 162, no. 3, pp. 233–245, 2003.

[28] S. Zhou, Y. Liu, and G. Wang, "The stability of predator-prey systems subject to the Allee effects," *Theoretical Population Biology*, vol. 67, no. 1, pp. 23–31, 2005.

[29] S. Krishna, "Conservation of an ecosystem through optimal taxation," *Bulletin of Mathematical Biology*, vol. 60, no. 3, pp. 569–584, 1998.

[30] K. S. Chaudhuri, "A bioeconomic model of harvesting a multispecies fishery," *Ecological Modelling*, vol. 32, no. 4, pp. 267–279, 1986.

[31] K. S. Chaudhuri, "Dynamic optimization of combined harvesting of a two-species fishery," *Ecological Modelling*, vol. 41, no. 1-2, pp. 17–25, 1988.

[32] M. Mesterton-Gibbons, "On the optimal policy for combined harvesting of independent species," *Natural Resource Modeling*, vol. 2, pp. 107–132, 1987.

[33] T. K. Kar and K. S. Chaudhuri, "On nonselective harvesting of a multispecies fishery," *International Journal of Mathematical Education in Science and Technology*, vol. 33, no. 4, pp. 543–556, 2002.

[34] T. K. Kar and K. S. Chaudhuri, "On non-selective harvesting of two competing fish species in the presence of toxicity," *Ecological Modelling*, vol. 161, no. 1-2, pp. 125–137, 2003.

[35] K. S. Chaudhuri and S. Saha Ray, "On the combined harvesting of a prey-predator system," *Journal of Biological Systems*, vol. 4, pp. 373–389, 1996.

[36] T. K. Kar, U. K. Pahari, and K. S. Chaudhuri, "Management of a prey-predator fishery based on continuous fishing effort," *Journal of Biological Systems*, vol. 12, no. 3, pp. 301–313, 2004.

[37] A. P. Gutierrez, "The physiological basis of ratio-dependent predator-prey theory: a metabolic pool model of Nicholson's blowflies as an example," *Ecology*, vol. 73, no. 5, pp. 1552–1563, 1992.

[38] H. R. Akcakaya, R. Arditi, and L. R. Ginzburg, "Ratio-dependent prediction: an abstraction that works," *Ecology*, vol. 79, pp. 995–1004, 1995.

[39] R. Arditi, L. R. Ginzburg, and H. R. Akcakaya, "Variation in plankton densities among lakes: a case for ratio-dependent models," *The American Naturalist*, vol. 138, pp. 1287–1296, 1991.

[40] C. Cosner, D. L. Deangelis, J. S. Ault, and D. B. Olson, "Effects of spatial grouping on the functional response of predators," *Theoretical Population Biology*, vol. 56, pp. 65–75, 1999.

[41] R. Arditi and A. A. Berryman, "The biological paradox," *Trends in Ecology and Evolution*, vol. 6, p. 32, 1991.

[42] P. A. Abrams and L. R. Ginzburg, "The nature of predation: prey dependent, ratio-dependent or neither?," *Trends in Ecology & Evolution*, vol. 15, no. 8, pp. 337–341, 2000.

[43] R. Arditi and L. R. Ginzburg, "Coupling in predator-prey dynamics: ratio-dependence," *Journal of Theoretical Biology*, vol. 139, no. 3, pp. 311–326, 1989.

[44] D. Xiao and S. Ruan, "Global dynamics of a ratio-dependent predator-prey system," *Journal of Mathematical Biology*, vol. 43, pp. 268–290, 2001.

[45] F. Berezovskaya and G. Karev, "AND R. ARDITI, Parametric analysis of the ratio-dependent predator-prey model," *Journal of Mathematical Biology*, vol. 43, no. 3, pp. 221–246, 2001.

[46] Y. Kuang, "Rich dynamics of Gause-type ratio-dependent predator-prey system," *Fields Institute Communications*, vol. 21, pp. 325–337, 1999.

[47] Y. Kuang and E. Beretta, "Global qualitative analysis of a ratio-dependent predator-prey system," *Journal of Mathematical Biology*, vol. 36, pp. 389–406, 1998.

[48] C. Jost and O. Arino, "AND R. ARDITI, About deterministic extinction in ratio-dependent predator-prey models," *Bulletin of Mathematical Biology*, vol. 61, no. 1, pp. 19–32, 1999.

[49] S. B. Hsu, T. W. Hwang, and Y. Kuang, "Global analysis of the Michaelis-Menten type ratio-dependent predator-prey system," *Journal of Mathematical Biology*, vol. 42, pp. 489–506, 2001.

[50] Y. A. Kuznetsov, *Elements of Applied Bifurcation Throry*, Springer-Verlag, New York, 2nd edition, 1998.

[51] J. Guckenheimer and P. Holmes, "Nonlinear Oscillations," in *Dynamical System and Bifurcation of Vector Fields*, Springer-Verlag, New York, 2002.

[52] P. Turchin, *Complex Population Dynamics*, Princeton University Press, Princeton New Jersey, 2003.

[53] F. Brauer, C. Castillo-Chavez, and C. Castillo-Chavez, *Mathematical Models in Population Biology and Epidemiology*, Springer, New York, 2001.

[54] R. P. Gupta and P. Cahndra, "Bifurcation analysis of modified Leslie-Gower predator-prey model with Michaelis-Menten type prey harvesting," *Journal of Mathematical Analysis and Applications*, vol. 398, no. 1, pp. 278–295, 2013.

[55] S. S. Askar, A. Ibrahim, and A. A. Elsadany, "A. Dynamics of a heterogeneous constraint profit maximization duopoly model based on an isoelastic demand," *Complexity*, vol. 2021, Article ID 6687544, 2021.

[56] S. S. Askar and A. Al-Khedhairi, "Further discussions of the complex dynamics of a 2D logistic map: basins of attraction and fractal dimensions," *Symmetry*, vol. 12, no. 12, p. 2001, 2020.

[57] J. Guckenheimer, P. Holmes, J. Guckenheimer, and P. Holmes, *Nonlinear oscillations, dynamical system and bifurcation of vector fields*, vol. 42, Springer-Verlag, New York, 1983.